Environment, Timing and Petrogenesis of a Middle Proterozoic Volcanic Suite: Port Victoria South Australia

Scott James Huffadine B.Sc.

Thesis submitted as partial fulfilment of the
Honours Degree of Bachelor of Science

University of Adelaide
Department of Geology and Geophysics
November, 1993

Grid reference
SI 54/12 Maitland Sheet
(1:250 000)

Supervisor: J D Foden

Abstract

The Middle Proterozoic volcanic assemblage at Pt. Victoria South Australia is representative of a subaqueous eruptive sequence intrusive to sediments which are likely to be of a deep water basinal origin. The felsic rhyodacites are characteristic of A-type granitoids, alkali enriched in incompatible elements and anorogenic. The basic amphibolites are tholeiitic in nature. Both rock types characterise an intra plate tectonic environment supported by incompatible element Y vs Nb and Y+Nb Vs Rb discrimination plots which indicate in the case of the rhyodacites that they originate in a within plate setting. The petrogenesis of the A-type rhyodacites is considered in light of current models including partial melting of a tonalitic to granodioritic source, a residual igneous source and Assimilation and Fractional Crystallisation (AFC). On the basis of trace element modelling and other indicators of fractionation, AFC of a mantle derived source is believed to best account for the observed A-type compositions. εNd values indicate a short crustal pre history and a dominant mantle component providing more support for AFC than either partial melting or a residual source. The volcanics at Pt. Victoria are common to much of the Proterozoic volcanic activity having close affinities to other suites of a similar time frame, the Moonta porphyry and Tidnamurkana volcanics. They also share the character that much of the activity between 1870 and 1500 Ma in South Australia and elsewhere in Australia are commonly A-type. The uniting theme for the above considerations is their implications to crustal growth in the Proterozoic. Was it a situation of recycling of existing Archean crust or was it generation of new crustal material by an alternative mantle source ? On the basis of tectonic environment, relation to other volcanics in the same time frame and petrogenesis by AFC from an initial mantle source, the evidence from Pt. Victoria indicates that the Proterozoic was a period of significant addition of new crustal material.

Contents

List of Tables, Plates & Figures.

Plate 1 Massive pink/red rhyodacite intruded by one of the dominant pegmatites.

Plate 2 Flow folded pink/grey rhyodacite showing characteristic flow folds.

Plate 3 Flow folds and bands in the rhyodacite.

Plate 4 Flow banding in the rhyodacite showing the characteristic flow foliation.

Plate 5 Gradational contact between the hyaloclastite jigsaw fit breccia on the right and metasediment on the left.

Plate 6 Layered metasediment showing alternating calc-silicate and quartzo feldspathic interlayers.

Plate 7 Amphibolites showing their pod like intrusive nature.

Plate 8 Early pegmatite North of the Jetty intruding the massive metasediments and showing sinuous folding.

Plate 9 Glomeroporphyryitic texture in breccis clasts showing agglomeration of plagioclase crystals X 10.

Plate 10 Biotite wraping around relic feldspar crystals defining a folitaion X 10.

Plate 11 Poikiloblastic muscovite in the metasediments with embayments of quartz crystals X 10.

Plate 12 Secondary calcite veining indicating fluid flow in the quartzofeldspathic interlayers X 10.

Chapter 1. Introduction

1.1 Introduction

The Gawler Craton covers an area approximately 600 by 800 km encompassing the Eyre Peninsula and the majority of the Yorke Peninsula, it is bounded to the east by the Adelaide Fold Belt and to the north by the Officer Basin. It is the largest of South Australia's basement provinces and contains units ranging in age from Late Archean to Middle Proterozoic . Since approximately 1450 Ma the area has remained stable apart from local epeirogenic activity (Fanning et al., 1988).The sequence of volcanic rhyodacites, hyaloclastite breccias and associated metasediments at Pt. Victoria lie on the poorly exposed eastern margin of the craton and have not been the focus of any major studies to date. Nevertheless the area has the potential to provide some insight into the processes which were acting on the Gawler Craton during the Proterozoic and can be expanded to include the Australian continent as a whole. These can be considered in terms of crustal generation, whether the crust was derived from the reworking of existing Archean and Proterozoic crust or if a mantle component was important. If a mantle component is involved, a question of its source region must be considered. In addition to this the tectonic environment in which this new crust is being generated is an important factor.

In order to resolve these processes in the context of what is seen at Pt. Victoria, it is the intention of this study to i) constrain the environment of deposition of the units on the basis of lithological characteristics and relationships; ii) Establish the tectonic environment which prevailed in the region by the use of geochemical discriminants common to particular tectonic settings; iii) Identify the source of the volcanics and in conjunction with this develop a petrogenetic model for the magma which gave rise to them. These aims will be supported by the use of major and trace element geochemistry, Rb/Sr and specifically Nd/Sm isotope geochemistry to constrain the timing of events and determine the extent of crustal contamination. Another aspect which will be explored is the fact that a number of felsic suites occur within specific time ranges in the Proterozoic and display characteristic geochemical fingerprints allowing comparison. Data obtained from SADME on a number of South Australian Proterozoic volcanics will be compared with the analysed data from those at Pt. Victoria and the Moonta Porphyry. Comparisons of the basic amphibolites will also be made in a similar manner to the felsic rock with other basic units from the Gawler Craton and other Proterozoic complexes.

1.2 Previous Investigations

Pt. Victoria is located approximately forty kilometres south of the widely studied Moonta-Wallaroo mining district (Figure 1.1) where the bulk of the work has concentrated on the associated copper mineralisation. Minimal work has been carried out on the geology of the Pt. Victoria area. The rhyodacites were described by Crawford (1965) as red feldspathic gneisses and paragneisses.

More recently Bone (1978) identified the basement on Wardang Island offshore from Pt. Victoria as, "metamorphosed volcanics of the andesitic suite" (Bone, 1978).
This study led to the recognition of the volcanics as a new stratigraphic sequence within the existing framework of the Gawler craton. Bone carried out Rb/Sr isotope geochemistry with a smaller component of major and trace element geochemistry on the rhyodacite basement units.

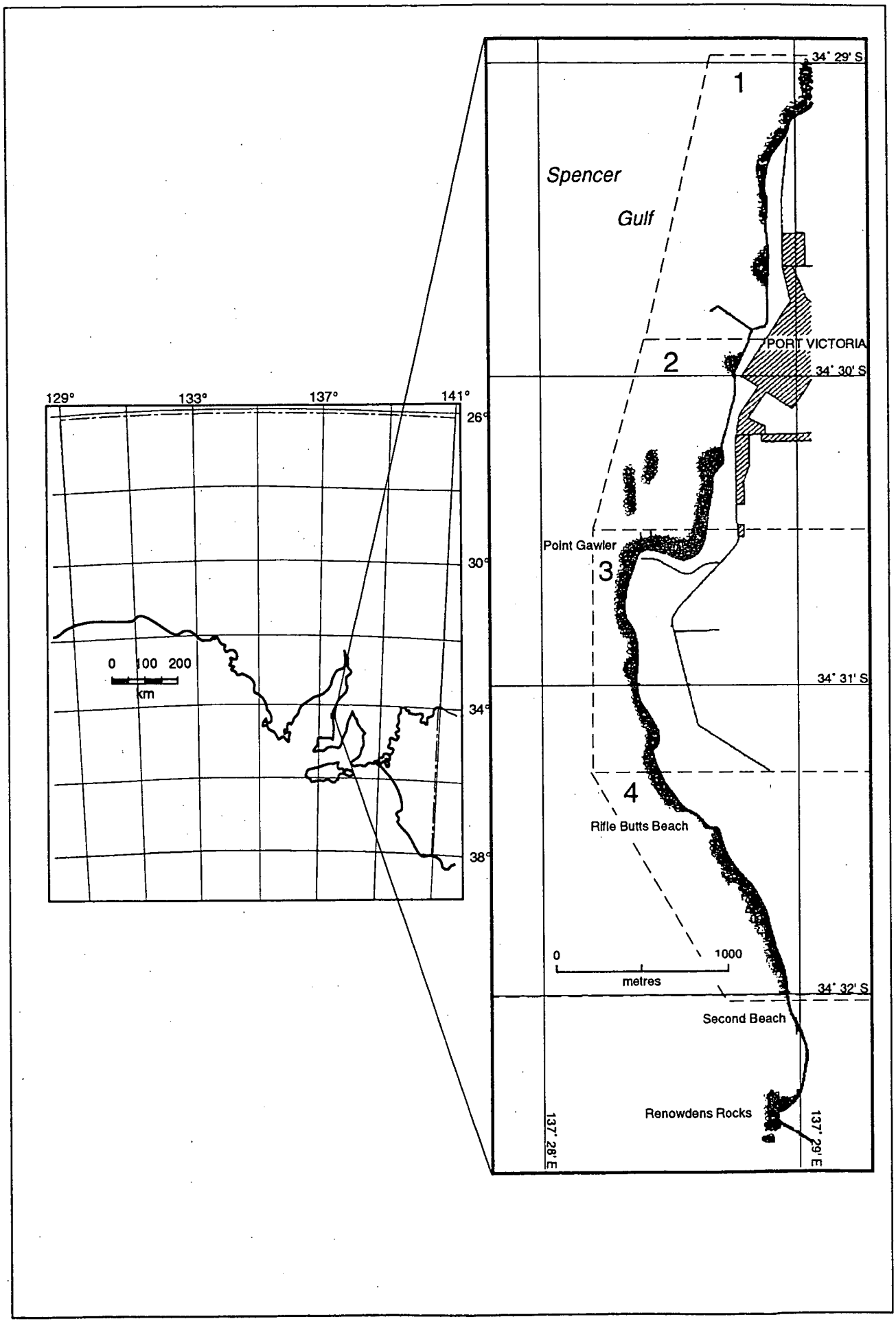

Figure 1.1 Locality map of the Pt. Victoria area.

Chapter 2. Regional Geology

Pt. Victoria is located within the Moonta Subdomain of the Gawler Craton, which is an extension of the Cleve Subdomain on Eyre Peninsula (Figure 2.1). Due to extensive Quaternary sediment cover, much of what is understood about the regional geology of the northern and central Yorke Peninsula has been determined from information around the Moonta-Wallaroo mining area It has been proposed by Parker (1990) that the region developed during the Kimban Orogeny as a distinct zone separate from events on Eyre Peninsula in the same time frame. This is based on the lithological variations between the dominantly clastic sediments of the Hutchison Group of Eyre Peninsula and the volcanic units on the Yorke Peninsula. The lithilogical variations led to the suggestion by Parker (1990) that the Moonta Subdomain may represent a volcanic arc or subduction zone which accreted onto the eastern margin of the Gawler Craton. He also suggests the tectonic regime may have been in the mode of Etheridge et al (1987) involving intra-plate ensialic rifting followed by subsequent underplating and accretion of Archean material to the Proterozoic crust.

Fanning et al. (1988) identify three major periods in the development of the craton, the Moonta Subdomain is associated with the second of these periods. Beginning in the Early Proterozoic it involved at least three periods of basin development with accompanying volcanism. Associated with this were episodes of intrusive granitic activity and deformation during the Kimban Orogeny (Fanning et al. , 1988). The Kimban Orogeny involved three periods of deformation, the last two D_2 and D_3 were experienced in the Moonta-Subdomain. D_2 is characterised by isoclinal folding with NW-SE trends and associated amphibolite facies metamorphism. D_2 has been dated by Webb et al. (1986) at approximately 1700 Ma on the basis of resetting events in rocks affected by this event. D_3, like D_2, has been characterised from examples in the Cleve Subdomain and involved open folding with the same trends as D_2. The age of D_3 has not been constrained as precisely as D_2, however it is likely that D_2 and D_3 were experienced more intensely in some regions and at different times in others. The basic time range of these can be seen in Figure 2.2. Webb et al (1986) consider that in most areas orogenic activity ceased by 1580 Ma and the region became stable at some time around 1400 Ma.

The rock units of interest in the region are the Doora Schist, a variable sequence described by Plimer (1980) as a " composite unit of mafic, pelitic and psammitic schists". The Moonta Porphyry is a brick red felsic porphyritic rock which has been dated using the U-Pb zircon method at 1741± 9 Ma (Fanning et al.,1988). Parker (1990) correlated the Moonta Porphyry on the basis of textural and deformational characteristics with the Wardang Volcanics which are located offshore from Pt. Victoria (Parker, 1990).

Plimer considers that the Moonta Porphyry conformably intrudes the Doora Schist. Also of importance in terms of heat sources for metamorphic events in the region, is the intrusion of the Tickera and Arthurton granites following the Kimban Orogeny. These are considered to be Middle Proterozoic equivalents of the Hiltaba suite on Eyre Peninsula, with the Arthurton granite dated at 1585±3 Ma (U-Pb) by Creaser (1989) (Hafer, 1991). The above mentioned units are unconformably overlain by a more extensive sequence shown in Figure 2.3. The Hutchison group is considered basal to the Doora Schist but this is only suggested and not observed.

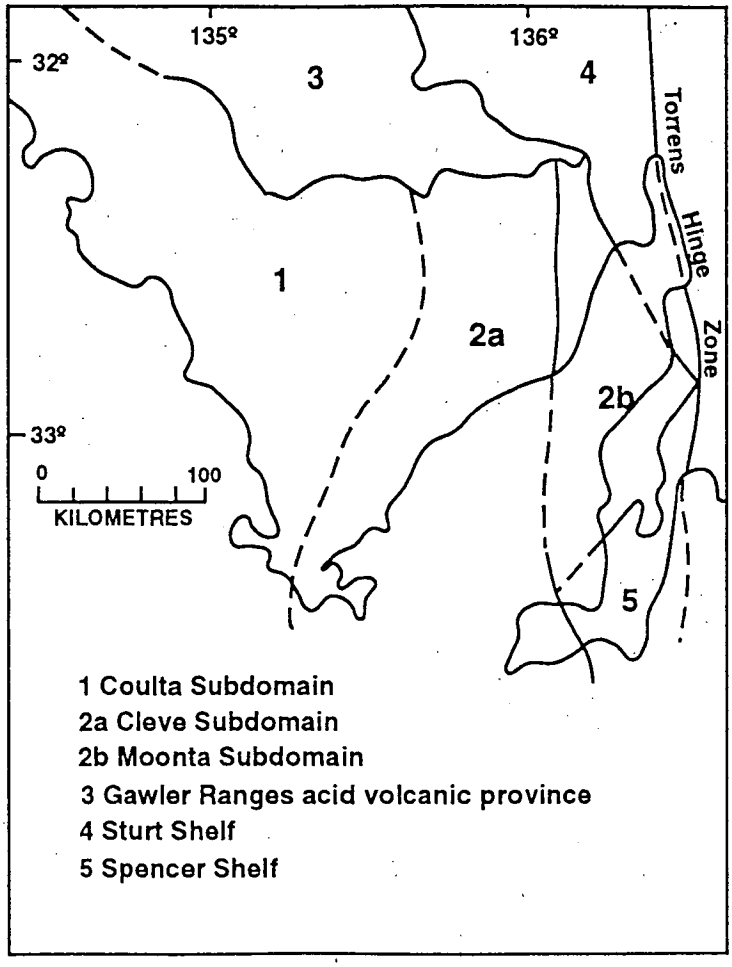

Figure 2.1 Tectonic subdivisions of the Gawler Craton (after Parker & Lemon,1982)

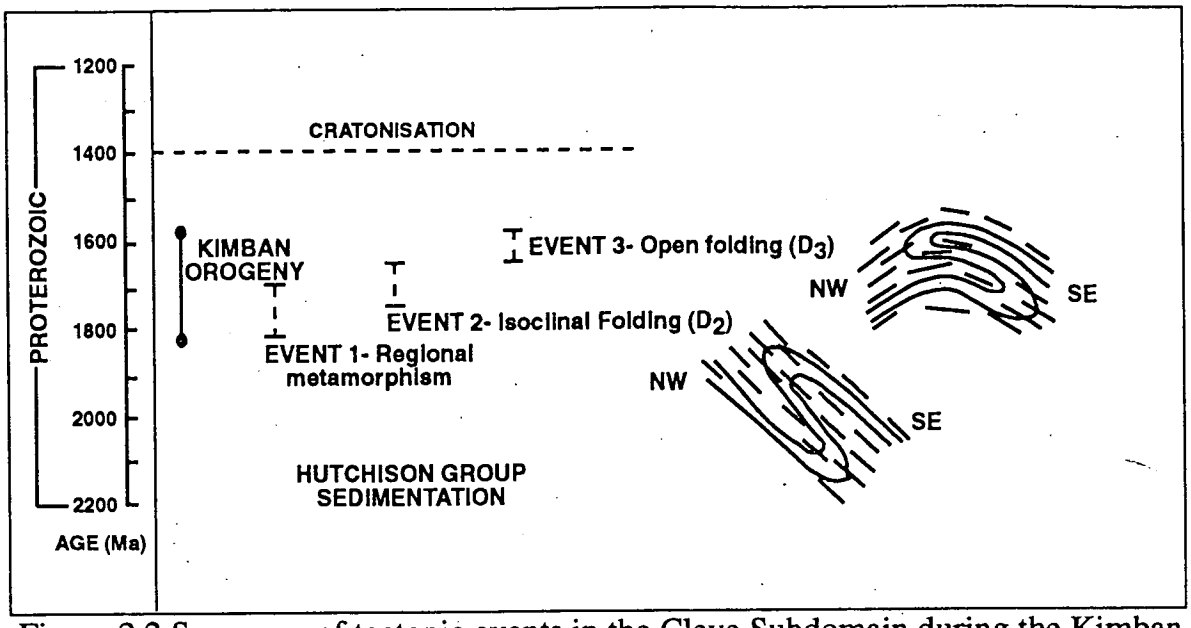

Figure 2.2 Summary of tectonic events in the Cleve Subdomain during the Kimban Orogeny. (from Parker & Lemon, 1982)

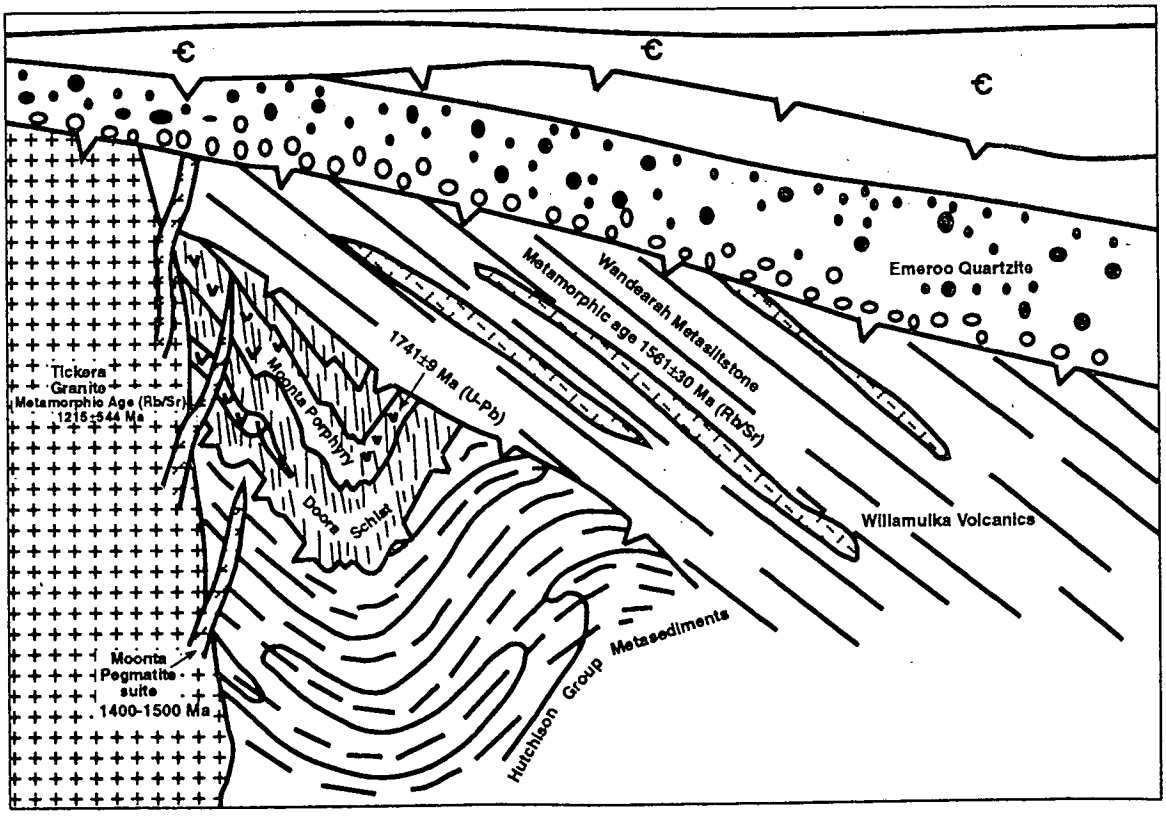

Figure 2.3 cross section of the units present in the Moonta Subdomain (after Parker in Plimer, 1980).

3. Local Geology

3.1 Introduction

The study area covered the previously recognised basement in and to the south of the township of Pt. Victoria representing a 6 kilometre coastal strip. The problem in this area like much of the northern part of Yorke Peninsula is the lack of outcrop resulting from an extensive cover of Quaternary and Recent sediments. The sequence at Pt. Victoria is represented by metavolcanic rhyodacites and intermediate breccias which intrude quartzofeldspathic and layered calc-silicate metasediments. The metasediments and volcanics are in turn intruded by amphibolite pods and pegmatite dykes. A model of the eruptive environment is developed on the character and relationships of the above mentioned units to one another. The region including the Pt. Victoria area has experienced deformation in the form of events D_2 and D_3 of the Kimban Orogeny. Metamorphism was associated with the deformation and at least two episodes i) of high grade amphibolite facies and ii) of retrograde metamorphism have been experienced. The rhyodacites and metasediments are considered the same as those documented by Bone (1978) on Wardang Island, the breccias are however unique to the Pt. Victoria area.

3.2 Rhyodacite

This is the dominant lithology in the area represented by a strongly jointed massive pink/red porphyritic rhyodacite (Plate 1) and pink/grey flow folded equivalent (Plates 2, 3 and 4). The gneissic character described by Crawford (1965) is seen in the massive unit and was also identified in the equivalent rhyodacites on Wardang Is. by Bone (1978) who interprets this as a result of metamorphic segregation of hornblende and biotite. These have reaction rims which are likely to be the result of oxidation of iron as both biotite and hornblende are ferromagnesian minerals. In hand specimen the massive rock shows anhedral Fe stained feldspars with some visible biotite and hornblende. The groundmass is aphanitic with petrography showing that it is microcrystalline.

The flow folded rhyodacites are chaotic in nature and trends in the folds are not consistent from outcrop to outcrop. They show a similar composition to the massive rocks with more visible biotite which defines a flow foliation. In hand specimen the feldspars show a random orientation and are not elongated. The groundmass is aphanitic and though it looks different to the massive rock, the geochemistry and gradational contacts in the field suggest they are the same rock.

3.3 Breccia

The breccias are like the rhyodacites, porphyritic but far more mafic in composition, having SiO_2 contents on average around 52.5 %. The clasts are angular indicating a rapid formation process such as quenching (Plate 5). While the breccia is dominantly formed in the intermediate rock type, it is observed in some areas to form in the flow folded rhyodacite. The flow fabric can be traced from clast to clast indicating in situ brecciation. The breccias occur as large sheets in more extensive out crop overlying the massive and flow folded rhyodacite. The contacts with the metasediments are gradational and conformable (Plate 5). Apophyses of breccia are found in zones within the rhyodacite supporting the intrusion of these through the breccia. In hand specimen the breccias are porphyritic with iron stained feldspars and a matrix which is coarser than the rhyodacites. Biotite and hornblende with minor quartz are the main matrix constituents. The breccia matrix itself is a fine grained quartz rich sediment which displays fine laminations varying in thickness up to 1cm however the majority are finer than this.

3.4 Metasediments

The metasediments are divided into two sub-units 1) a massive unit and 2) a layered unit. The massive sub-unit is a foliated and undifferentiated quartzo-feldspathic greywacke. The unit is approximately 15 metres thick and is considered to be intruded and overlain by the rhyodacites with the contact between the two being inferred. In hand specimen the massive unit consists of quartz, feldspar and biotite with larger muscovite crystals. The biotite defines a foliation in the rock. Plimer (1980) in a description of the geology of the Moonta area describes the Doora schist as an enigmatic rock type which has a number of mappable assemblages. One of these is a feldspar-quartz-biotite assemblage and it is considered that the massive unit is Doora schist equivalent.

The layered unit consists of alternating calc-silicate and quartzo-feldspathic bands which show an almost rhythmic repetition (Plate 6). The calc-silicate bands range in thickness from 2 to 10 cm and contain quartz, amphibole, minor epidote and carbonate.The quartzo-feldspathic layers also have a major component of amphibole which defines a foliation most likely produced during metamorphism. The unit dips steeply to the west, and while only seeing identifiable fold structures at two sites the layers do show a general warping.

3.5 Amphibolites

The amphibolites are a prominent feature of the section, intrusive to both the metasediments and the rhyodacites. They occur as pods or rafts of varying sizes (Plate 7), rather than as obvious dyke structures as identified by Bone (1978) on Wardang Is. An extensive outcrop of amphibolite which begins immediately south of the jetty and extends for some 150 metres could represent a large dyke like structure, but in accordance with the other amphibolites in the area it is most likely the site of more voluminous intrusion of basaltic material. A similar outcrop is seen ~1 km to the south of the present study area at Renowdens Rocks (see Fig. 1.1). The amphibolites are foliated and considered to have been emplaced in a similar time frame to the volcanics, but prior to D_2 the first deformation event in the area.

3.6 Pegmatites

There is a dominant pegmatite suite which have a similar WNW-ENE orientation. They are reddish in colour and contain large feldspar phenocrysts up to 4cm and smaller proportions of quartz. This reddish colour has been noted by Plimer (1980) in relation to the Moonta pegmatite suite which intrude the Moonta porphyry and are described as transgressive red pegmatites. The pegmatites cross cut the volcanics (Plate 1) and metasediments and are considered to be the youngest feature in the area on this basis. It is likely that the Pt. Victoria pegmatites are related to the Moonta suite, however no age dating was carried out so this can only be considered a possibility. There is another pegmatite to the north of the jetty intruding the metasediments which runs roughly N-S which differs compositionally to the major suite. It has much smaller feldspar crystals, quartz and large platy biotite and while still dyke like, it pinches out to narrow ends which are sinuous (Plate 8). From these observations it is obvious that they are different to the major suite and suggests two stages of pegmatite intrusion

3.7 Model of eruptive environment

The lithological relationships in the volcano-sedimentary sequence at Pt. Victoria suggest the intrusion of the intermediate and rhyodacite lavas/magmas in a subaqueous environment. The presence of hyaloclastite breccias supports the subaqueous extrusion of the lava. While the exact depth at which eruption occurred cannot be determined some constraints can be placed on this. Hyaloclastites result from the non explosive fragmentation of an erupting magma, the reason for the non- explosive nature is that the hydrostatic pressure of the overlying water column prevents the expansion of the erupting body of lava (Cas, 1992).

Cas (1992) has divided submarine silicic lavas into three main types i) Lava domes ii) laterally extensive lava flows and iii) largely intrusive high level domes (cryptodomes) which intrude the sediment pile and hardly breach the surface. The association of hyaloclastite breccias and the more massive and flow folded rhyodacite at Pt. Victoria most closely equates

to this last type (Figure 3.1). Cas (1992) suggests that the cryptodomes are fed by dyke systems which intrude a similtaneously growing pile of hyaloclastite produced from the quenching and autobrecciation on the outer margins of the erupting magma. The subsequent association of rock types show a progression from a massive lithic crystallised core to flow banded obsidian rim to in situ jigsaw fit fractured breccias. This has been documented in both Miocene and Archean examples. A similar gradation from massive to flow folded rhyodacite to an intermediate hyaloclastite breccia is evident at Pt. Victoria .

The cryptodome model involves only partial or no breaching of the sediment surface into which they are intruding. In such a situation the water saturated sediments which are being intruded can cause significant quench fragmentation producing hyaloclastites on the margins of the cryptodome. The fact that the sediments are older than the intrusive rhyodacites has been established by the use of Sm-Nd isotopes which demonstrates that the sediments are not sourced and are older than the rhyodacites (figure 3.2). A characteristic feature of in situ hyaloclastites is the occurrence of jigsaw fit textures between groups of clasts. The jigsaw or curvlinear clasts characteristic of hyaloclastites can be seen at Pt. Victoria and results from the above mentioned rapid quenching. As mentioned hyaloclastite can be a common product where magmas intrude and pass through water saturated or unconsolidated sediments, the massive undifferentiated unit possibly of deep water origin could represent such sediments.The contacts between the sediments and intrusives are gradational, a situation which is seen between the sediment and hyaloclastite at Pt Victoria.
The environment of deposition when considered in light of the character of the metasediments and the processes occuring in the region at the time of intrusion is likely to be a marginal basin, similar in nature to that into which the extensive early Proterozoic Hutchison Group was deposited.

3.8 Structure

The rocks at Pt Victoria were subjected to two periods of deformation related to events D_2 and D_3 of the Kimban Orogeny. D_2 and D_3 have been characterised by Parker and Lemon (1982) in the Cleve sub-domain which is divided into two subgroups, 2a which incorporates the area on the Eyre Peninsula and 2b which is the Moonta subdomain and includes the Pt. Victoria area(Figure 2.1) . The initial deformation was D_2 which was a major folding event producing tight to isoclinal folds. These are similar in form and range in size up to macroscopic structures (Parker and Lemon, 1982). The steep dips of the layering in the metasediments and flow foliation as well as the alignment of biotite in the metasediments are seen to be a result of this isoclinal folding. The layered metasediments bend around before contact is lost in all areas of outcrop. It is proposed on the basis of this that these are on the limb of a major fold. The fold structures and warping may be parasitic features associated with compensation of excess strain on the limbs of the fold.

The second deformation is not as obvious, however it has been documented in the region on Wardang Island by Bone (1978) and in the Moonta Porphyry by Hafer (1991).This deformation (D_3) was characterised by open folds with the development of mylonites on the Eyre Peninsula. D_3 folding was characteristically upright and open and are similar to parallel in form (Parker and Lemon, 1982). The folds seen at Pt Victoria are upright and similar but much tighter than those described from the Cleve Subdomain, they may however be associated with this deformation.

3.9 Metamorphism

Parker and Lemon (1982) identify a number of episodes of metamorphism within the Cleve Subdomain associated with the Kimban Orogeny. The Moonta subdomain experienced two of these events associated with D_2 and D_3 which occurred following its proposed time of generation. The rocks at Pt Victoria have been metamorphosed to at least mid amphibolite facies. Evidence for this is the presence of green-brown hornblende, dominant in the amphibolites, metasediments and present in the rhyodacites. The fact that the hornblende is seen in an alignment with biotite suggests its development due to metamorphism synchronous with deformation. Amphibolite facies metamorphism has been documented for the first two events of the Kimban but it is considered that this period of metamorphismn is associated with D_2. Parker and Lemon op cit. note that following D_2 the metamorphic grade in the region began to decrease and the third deformation took place under retrograde conditions. Evidence for this is the presence of common retrograde mineralogies such as sericite, chlorite seen after biotite, epidote and the large poikiloblastic muscovite seen in the massive unit which is considered to be a retrograde product. The silicification of the rocks indicates that a hydrothermal event has occurred, possibly in association with D_3. This is evident in the breccia matrix which could have chanelled any fluids and displays elevated SiO_2 contents between 79-86%. The presence of quartz veins representative of silica rich fluids and the abundance of pegmatites suggests that this event has some relationship to these. Further support for fluid flow is provided by the presence of calcite in minor amounts which is often deposited from late stage magmatic solutions.

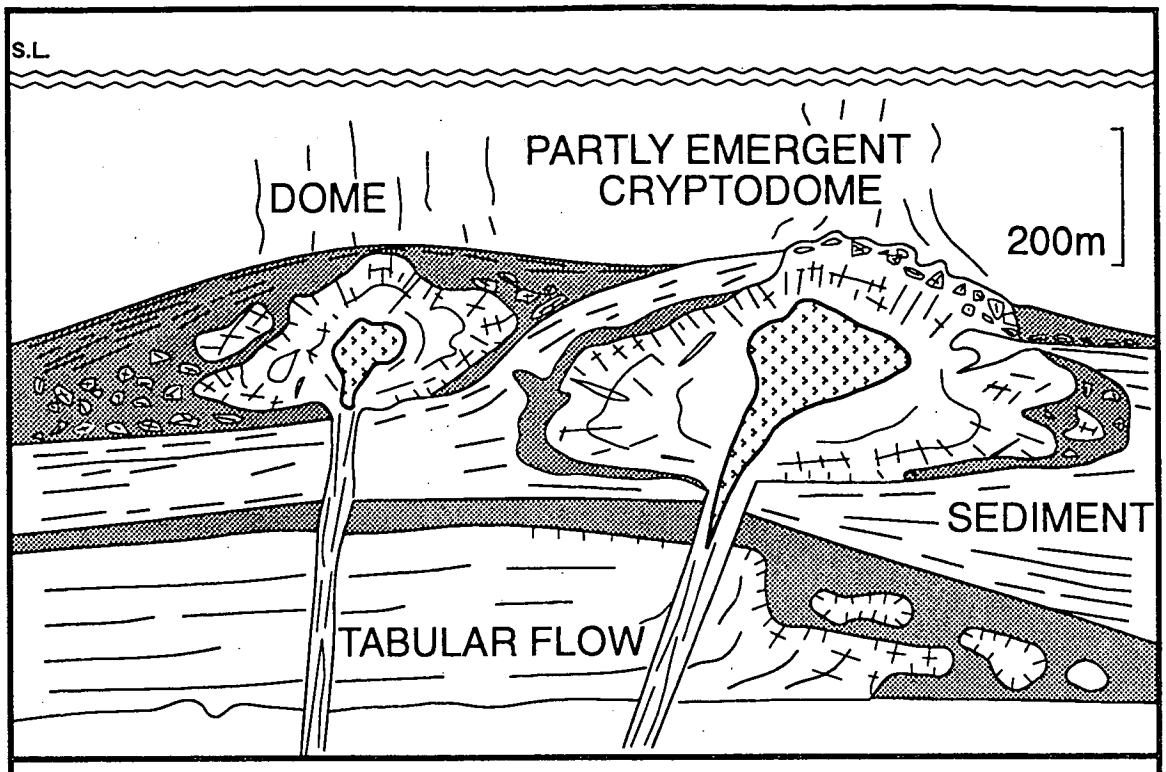

Figure 3.1 Model of development of doming and brecciation on outer margins of a body of magma intruding wet unconsolidated sediments. (after Cas, 1992)

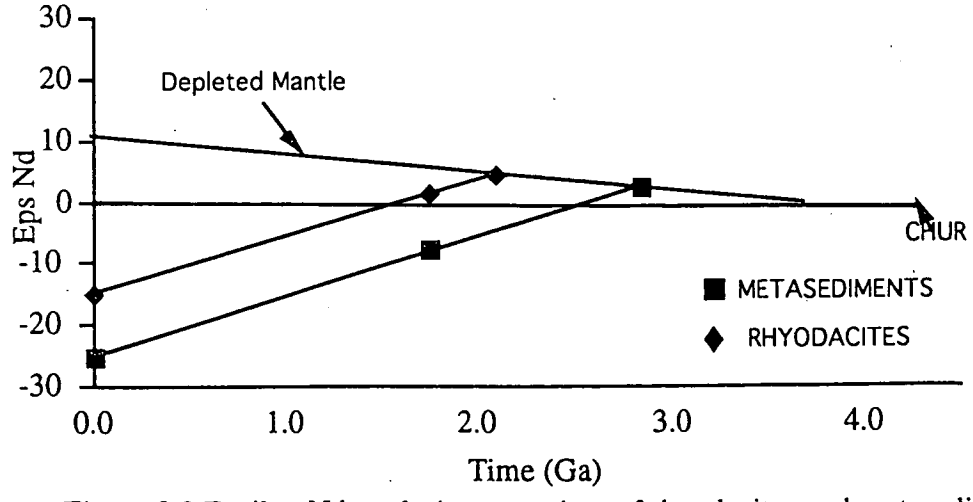

Figure 3.2 Epsilon Nd evolution over time of rhyodacites and metasediments

Plate 1 Massive pink/red rhyodacite intruded by one of the dominant pegmatites

Plate.2 Flow folded pink/ grey rhyodacite showing characteristic flow folds

Plate 3 Flow folds and bands in the rhyodacite

Plate 4 Flow banding in the rhyodacite showing the characteristic flow foliation.

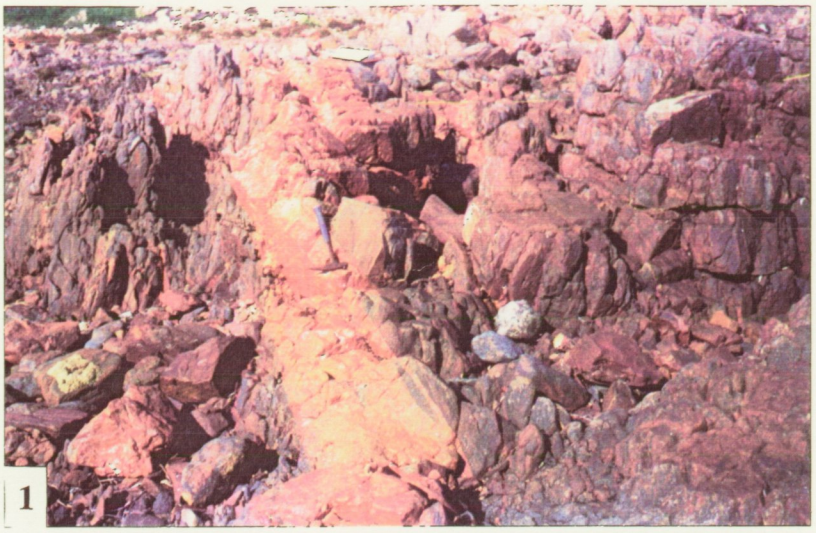

1

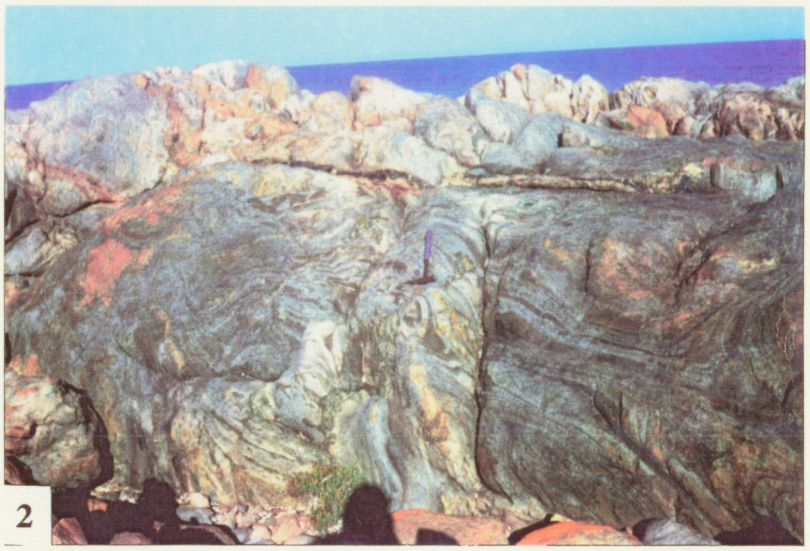

2

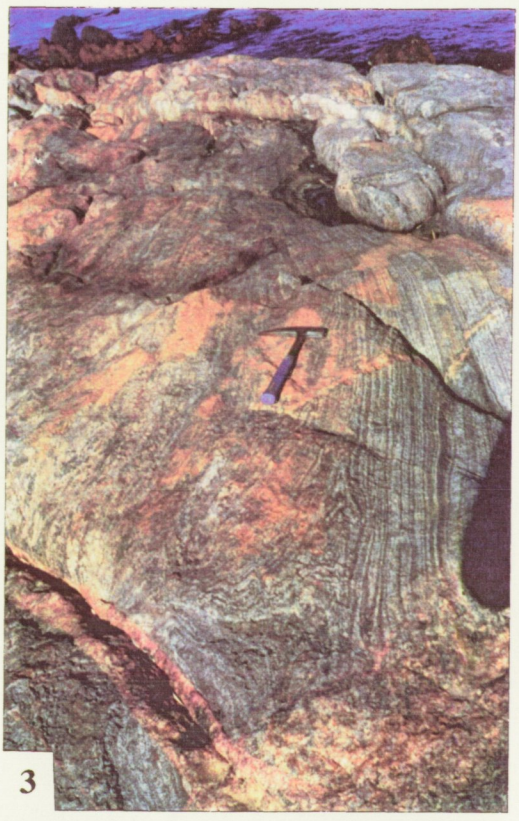

3

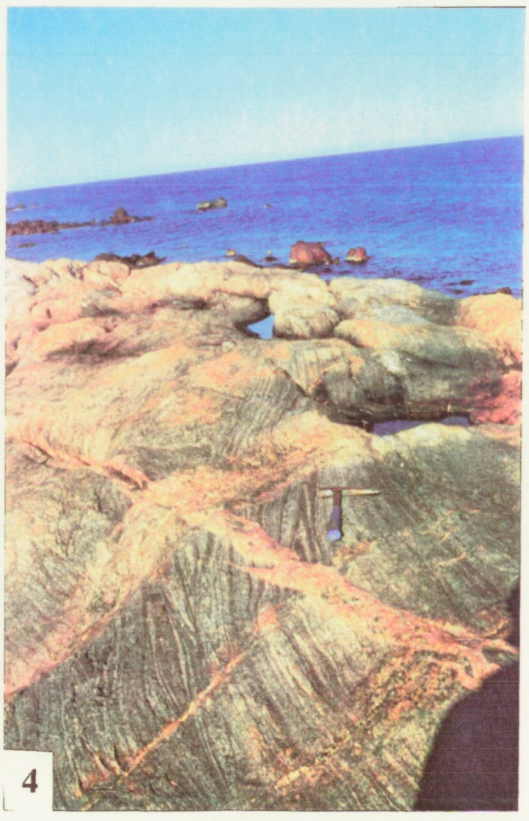

4

Plate 5 Gradational contact between the hyaloclastite jigsaw fit breccia on the right and metasediment on the left

Plate 6 Layered metasediment showing alternating calc-silicate and quartzo feldspathic interlayers

Plate 7 Amphibloites showing their pod like intrusive nature

Plate 8 Early pegmatite North of the Jetty intruding the massive metasediments and showing sinuous folding

5

6

7

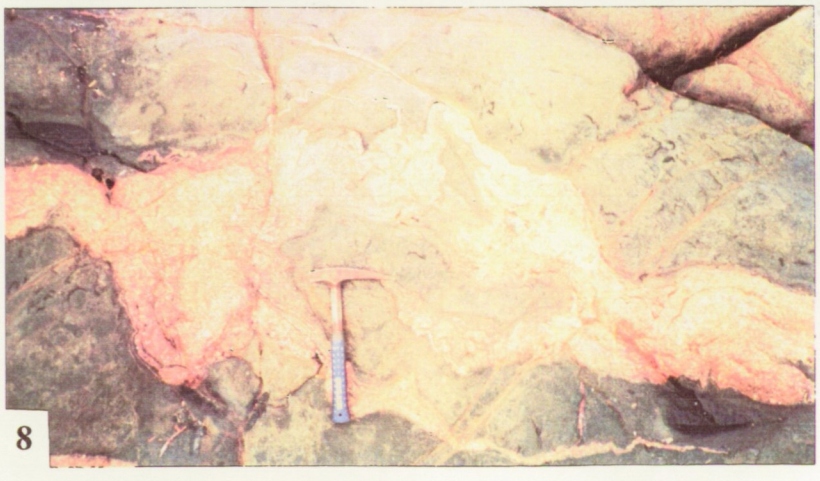

8

Plate 9 Glomeroporphyritic texture in breccia clasts showing agglomeration of plagioclase crystals. X 31

Plate 10 Biotite wrapping around relic feldspar crystals defining a foliation. X 31

Plate 11 Poikiloblastic muscovite in the metasediments with embayments of quartz crystals. X 31

Plate 12 Secondary calcite veining indicating fluid flow in the quartzo -feldspathic interlayers. X 31

Chapter 4. Petrography

4.1 Introduction

The purpose of this section is to provide an insight into the mineralogy of the various lithologies found in the Pt. Victoria section. In addition to this, evidence for the environment of deposition, metamorphism and deformation can be determined by textures, structures and minerals which cannot be discerned in hand specimen. More detailed thin section descriptions are recorded in Appendix 1.

4.2 Rhyodacites

A phenocryst assemblage composed of feldspars represented by microcline and plagioclase characterise this is a porphyritic rock. The feldspars are anhedral and range in size from 1-4 mm and show differing degrees of alteration by sericite. The matrix is extremely fine grained and may be a product of devitrification of glass. A common texture in older glassy rocks which have been devitrified is a granophyre stage, occurring as fine grained roughly equidimensional recrystallised aggregates of quartz and feldspar (Cas and Wright, 1987). This could account for the observed textures in the rhyodacites. The matrix is made up of microcline and plagioclase, occurring as anhedral to subhedral crystals ≤ 0.3 mm.

Quartz is of a similar size to the feldspars and composed of rounded subhedral crystals displaying undulose extinction. Biotite is seen as anhedral bladed and prismatic crystals which are ≤ 0.5 mm. Hornblende is present but its occurrence in the mode is variable from sample to sample. Together biotite and hornblende wrap around relict feldspar phenocrysts defining a metamorphic foliation. (plate 10). Opaques are represented by magnetite. Other accessory minerals found in trace amounts are apatite, fluorite and rutile. Sphene is only found in one of the sections as a minor component.

4.3 Amphibolites

The amphibolites are dominated by andhedral to subhedral crystals of hornblende varying in size up to 2mm and anhedral to subhedral plagioclase crystals 0.5-3mm. All of the samples described had been altered which is evident by the alteration of the feldspars to sericite. Biotite occurs as lathes of $\leq$ 1mm. Chlorite was obvious in one section occurring as radiating aggregates forming after biotite. Sphene is a common mineral and occurs as subhedral crystals $\leq$ 2mm and is associated with the opaques which form cores to the crystals. Other minor accessory minerals are small anhedral quartz crystals which show overgrowths. Apatite and rutile are also present but are only seen in trace amounts.

4.4 Breccia clasts

The clasts are porphyritic with an obvious magmatic origin. The phenocryst assemblage consists of microcline with minor plagioclase which are all anhedral and range in size from 2-4mm. The majority of these are heavily altered to sericite. Some of the phenocrysts form agglomerations indicative of a glomeroporphyritic texture (plate 9). This is a common texture in porphyritic volcanic rocks supporting the magmatic origin of this rock .

The matrix is fine grained and contains equigranular quartz defining "120 degree triple points". Anhedral crystals of microcline and plagioclase up to 1mm represent a major proportion of the matrix. Biotite is also prominent occurring as single anhedral crystals and aggregates up to 1mm. Hornblende is a minor component and occurs with the biotite.

Quartz is also present in the matrix as rounded subhedral crystals of 0.1-0.3 mm. Sphene occurs as subhedral grains indepedently and after pyrite and magnetite. Pyrite and magnetite both occur in minor proportions as overgrowths on the feldspar phenocrysts. Other minor phases are allanite replaced by chlorite, and epidote which rims the allanite. Euhedral crystals of apatite, fluorite and calcite are also present in the breccia clasts.

4.5 Breccia matrix

This is a fine grained siliceous sediment with rounded anhedral quartz crystals showing undulose extinction. Microcline occurs as small anhedral crystals ranging in size up to 0.7mm. Biotite forms as bladed crystal which do not show any preferred orientation, there is some alteration of these to epidote. Magnetite is an accessory mineral with crystals of $\leq$ 0.5mm. Other accessory phases are epidote, apatite and fluorite.

4.6 Metasediments

4.6.1 Massive sub-unit

The massive metasediment in section is quartzo-feldspathic, quartz is seen as large poikilitic anhedral crystals containing smaller quartz crystals. The feldspars are anhedral crystals of microcline which are $\leq$ 1mm and show some minor sericitisation.

Biotite is also a major constituent occurring as bladed and subhedral crystals showing an alignment defining a foliation. Hornblende is not common but it is also aligned and occurs as subhedral crystals.

Muscovite is present as large anhedral crystals ranging in size from 2-4mm. The muscovite also displays poikiloblastic textures possibly the product of a late stage retrograde reaction (Plate 11). Accessory minerals seen are opaques $\leq$ 0.3mm and apatite occurs as round euhedral crystals approximately 0.2 mm in size. Zircons occur as inclusions in the biotite and rutile is seen in trace amounts.

4.6.2 Layered sub-unit

Calc-silicate Layer. The calcsilicate rocks are dominated by large anhedral crystals of scapolite common in hydrothermally altered rocks. The scapolite shows a poikiloblastic texture with quartz inclusions. Small rounded and large anhedral crystals of quartz up to 1.5 mm form a major component. Clinopyroxene also occurs as subhedral crystals up to 4 mm and is replaced by hornblende. The hornblende forms dark green pleochroic rims around the cpx. Calcite is one of the major accessory minerals with sphene and apatite crystals also present in trace amounts.

Quartzo-feldspathic interlayer. The dominant component in the interlayer is anhedral microcline up to 0.5 mm in size. Hornblende occurs as subhedral crystals ranging in size up to 1 mm. Quartz is present as rounded subhedral crystals, however it is much less abundant than feldspar and hornblende. Accesory minerals are calcite which seems to be secondary occurring as discrete crystals and in veins (plate 12) and sphene is the other major accessory minerals.

Chapter 5. Major and Trace Element Geochemistry

5.1 Introduction

The aim of this section is to characterise the geochemical aspects of the lithologies present in the Pt. Victoria area and determine the genetic character of the volcanics and possible source rocks for the metasediments. In addition to this the tectonic environment which prevailed at the time of deposition will be considered by the use of tectonic discrimination diagrams.The relationship of these to the processes affecting the composition of the rocks will be elaborated on in the petrogenesis chapter.Geochemical analysis was carried out for major and trace elements using the X-ray Fluorescence technique (XRF) on a Phillips PW 1480 spectrometer, results are compiled in Appendix 2.

5.2.1 Rhyodacites

Plotted on a Nb/Y vs. SiO_2 discrimination diagram (Figure 5.1), the Pt. Victoria samples plot on and below the boundary of rhyodacites and rhyolites but the majority lie within the rhyodacite field. All of the samples are alkaline with high Na_2O+K_2O values (avg. 7.18 wt. %), they also have an $Al_2O_3/(K_2O+Na_2O+CaO)$ ratio >1 which classifies them as peraluminous. Reasonably high SiO_2 values range from 67.46 - 72.11 wt. %. Other elements which are high are Na_2O (avg. 4.12 wt. %) and K_2O (avg. 3.06 wt. %) which together impart the alkalic nature to the rock. In the trace elements the rhyodacites show enrichment in a number of the more incompatible elements and rare earth elements (REE) such as Zr (avg. 557 ppm), Y (avg. 76 ppm), Nb (avg. 38.2) and Ce (avg. 117.6 ppm). In general they are characterised by high incompatible elements, light rare earth elements (LREE) and heavy rare earth elements (HREE) and an average Ce/Y ratio of 1.55. The implications of these to petrogenesis of the rocks will be referred to in a later section.

The major and trace element features substantiate the classification of the rhyodacites as A-type granitoids, alkaline and anorogenic as first described by Loiselle and Wones (1979). A-type granites can be recognised on the basis of their chemical composition, high SiO_2, Na_2O+K_2O, Zr, Nb, Ga, Y and Ce with low Sr and CaO (Whalen et al. 1987 and Collins et al. 1982). Both these authors recognise the high Ga/Al ratios in A-type rocks as being highly diagnostic with Whalen et al. developing a method of discrimination using Ga/Al vs. various incompatible elements. The relationship between Ga and Al can be expressed more simply by Figure 5.2 which is a variation plot of Al_2O_3 vs. Ga employed by Collins et al. (1982) to discriminate A-type granites. The Ga/Al ratio is still a very useful discriminant with most A-type rocks being greater than 3, the Pt. Victoria rhyodacites have

an average of 3.09. The high Ga/Al ratios provides evidence that the melt which generated the rhyodacites was of a high temperature. Fluorine in aluminosilicate melts causes Ga to be retained because Ga and F complex in reaction which occurs and is stable at high temperatures. As a result, at higher temperatures during the generation of the dry A-type melt, Ga is retained in preference to Al because Al only complexes with F in water saturated melts. Chlorocomplexes of Ga and Al are not stable at higher magmatic temperatures and therefore do not affect the Ga/Al ratios (Collins et al.1982). Further support for a high temperature melt is substantiated by the large proportion of Zr in the rocks. Zr is incompatible at high temperatures and more compatible at lower temperatures where it is removed from the melt (pers. comm. J. Foden ,1993).

5.2.1 Breccia Clasts

The breccia clasts when plotted on figure 5.1 fall within the fields of trachyandesite and sub-alkalic basalts, however they do not show any relationship with these genetic groups. They have intermediate an SiO_2 composition (avg. 53.25 wt.%), the Al_2O_3 values are high at an average of 20.28 wt. % as is Fe_2O_3 (avg. 8.23 wt.%). Na_2O and K_2O with 5.3 and 4.76 wt.% respectively are also high. However the trace elements of the breccia clasts are distinctive with very high values for numerous elements, Y (avg. 88.35 ppm), Zr (avg. 876.5 ppm), Nb (avg.50.5 ppm), Ga (avg.43.4 ppm), Ce (avg. 207.5 ppm), Nd (avg. 100 ppm) and La (avg.115.5 ppm). While they are high in incompatible and LREE they do not show the same enrichment in V, Cr and Ni which are much higher in the amphibolites and presumed to be derived directly from the mantle. The relationship of the breccia clasts to the other igneous rocks is obscure however their petrogenesis in relation to the amphibolites and rhyodacites will be addressed in the section on petrogenesis.

5.2.3 Amphibolites

The amphibolites which are considered to be the products of metamorphosed basalts are interpreted on the basis of their geochemistry to be tholeiitic in character. They are moderately oversaturated and contain quartz with large amounts of hypersthene in the norm. The tholeiitic origin of the amphibolites is further supported when plotted on figure 5.3 showing the Alkali index (A.I.= Na_2O+K_2O/SiO_2-43*0.17) versus Al_2O_3 wt. % where all samples fall within the field of tholeiitic basalts. They also lie within the field of sub-alkalic basalts on figure 5.1. The major element geochemistry supports the above interpretation, with relatively high SiO_2 content (avg. 49.5 wt.%). The Al_2O_3 composition (avg. 14.18 wt.%) is consistent with tholeiites which commonly contain 12-16 % Al_2O_3, while calc-alkaline basalts contain 16-20% Al_2O_3 (Wilson, 1987). CaO values are also high (avg. 9.5 wt.%) consistent with the higher values found in the rhyodacites. In contrast to the above values the amphibolites are low in Na_2O and K_2O (avg. 2.36 and 1.28 wt %) respectively. The trace element composition displays higher concentrations of the compatible elements such as V (avg. 367.75 ppm) and Sr (avg. 206 ppm) with a Ga

content similar to the rhyodacites (avg. 21.625 ppm). U is the most obvious example of lower levels of all the trace elements, the average crustal content of U is around 3 ppm and the amphibolites have an average abundance of .3 ppm which is below the detection limit. Thorium is closely related to U and has similar low levels with an average of 2.7 ppm.

5.2.4 Pegmatites

The dominant suite of pegmatites are regarded as a late stage event because of their cross cutting nature in outcrop. Because of the nature of pegmatites, resulting from late stage residual fluids produced by the dewatering of granitic melts, they may become enriched in various trace elements. Rb is high (avg. 443.1 ppm) which can substitute for K in feldspars. Nb is also high with an average of 41 ppm but sample 26 at 6 ppm brings this average down. Ga is once again high but this is a common feature of all the rocks in the area. On the whole the majority of the trace elements are relatively low. Sample 26 representing the pegmatite mentioned earlier as compositionally different shows differing values for many elements. This in association with the field relationship suggests two stages of pegmatite intrusion, one pre and one post deformation.

5.2.5 Metasediments

The metasediments do not show any geochemical relationship with the volcanic rocks present which would negates the possibility of the rhyodacites or breccias sourcing the sediments. The incompatible trace elements such as Zr, Nb and Y have values which lie between the amphibolites and rhyodacites. Incompatible elements would be expected to remain unaffected by the processes leading to the sediment formation.
The major element characteristics of the massive unit are similar to those of the quartzo feldspathic interlayers between the calc-silicates. The massive unit and interlayers show slightly lower K_2O and CaO while the calc-silicates are much higher in CaO with more K_2O. In trace element concentrations all are found to be similar with Rb higher in the quartzo-feldspathic layers. Ba is variable throughout possibly due to its mobility during fluid flow. The overall similarity between interlayered bands and the more massive unit would seem to suggest that the calc-silicate is the product of alteration of a more CaO rich sections in the sedimentary pile.

5.3 Implications of geochemistry to tectonic setting

The specific tectonic setting in which a magma is generated can be determined by the use of discrimination diagrams based on the character of magmas from known settings. This is done using dominantly immobile elements, such as Zr, Ti and Y all considered to be resistant to the effects of metamorphism and alteration. Many of the rocks used to develop these tectonic

discrimination diagrams are Phanerozoic in age and the applicability of these to Proterozoic rocks must be considered. Because the processes involved in magma generation in the Archean and Proterozoic are not fully understood as they are for Phanerozoic and modern settings, they are considered to have been different. This led Pearce and Cann (1974) to the conclusion that for Proterozoic basic volcanic rocks the results gained from discrimination diagrams should be treated with a certain degree of reservation. In terms of tectonic discrimination for granitic rocks Pearce et al. (1984) consider that the processes in the PreCambrian were different and would have affected some parameters used in the discrimination diagrams. However they can still be applied to Proterozoic rocks as they are to Phanerozoic rocks (Pearce et al., 1984).

5.3.1 Rhyodacites

The 11 Pt. Victoria rhyodacites and 4 samples of Moonta Porphyry were plotted on i) Y vs. Nb and ii) Nb+Y vs. Rb discrimination diagrams after Pearce et al (1984), Figures 5.4 and 5.5. All samples plot in the within plate granite fields on both the diagrams. Because of the alteration in the area the plots use the less mobile elements to negate the effects of these processes. The within plate granites are considered by Pearce et al (1984) to fall in the alkalic suites according to Peacocks (1954) alkali-lime index and by definition fit the criteria for A-type granites. Pearce op cit. apply their discrimination diagrams to the petrogenesis of the rock types being considered on the basis of the boundaries between the contrasting types of granites. It is assumed that the within plate granites originate from areas of the mantle which are enriched in incompatible elements in relation to the bulk mantle composition (Pearce et al, 1984). The enrichment of incompatible elements as seen in section 5.2.1 would support this assumption.

5.3.2 Basic rocks

The trace element data from the amphibolites was also plotted on discrimination diagrams in an attempt to constrain the tectonic setting they were originally generated in. Because of the metamorphism and alteration experienced at Pt. Victoria, the discrimination diagrams were based on the less mobile elements as suggested by Pearce and Cann (1973). Figure 5.6 and 5.7 show that the amphibolites plot in the ocean floor basalt field, this was also the case for amphibolites of a similar time range from the Middleback Ranges, Eyre Peninsula (pers. comm. D. McKeown, 1993). Another aspect of the rocks which could be determined was if they were tholeiitic or alkalic in character. In order to determine thr tholeiitic or alkalic nature of the rocks the Y/Nb ratio was calculated. All of the amphibolites were greater than 3 which in the case of ocean floor basalts is indicative of tholeiitic rocks. Because the rhyodacites are indicative of an intra-plate setting it would be expected that the basalts would also plot in a similar field indicating a divergent continental setting. However as mentioned the results of this type of discrimination diagrams with regard to PreCambrian should be treated with reservation. An additional factor is the dominance of sphene, opaques (titanomagnetite?) and rutile in the petrography may indicate that Ti has been mobile (Pearce & Cann, 1973). The fact that Ti is

used in both the discrimination diagrams and may have been preferentially partitioned into these accessory phases suggests the discrimination of the amphibolites is not as conclusive as it was for the rhyodacites.

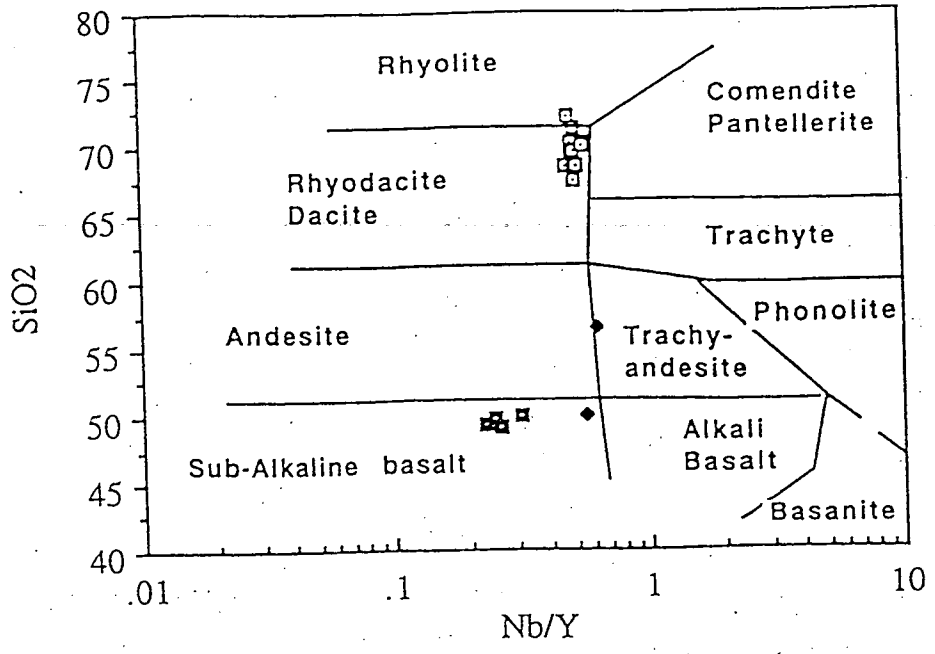

Figure 5.1 Nb/Y versus SiO_2 rock type discrimination diagram. (open squares -rhyodacites, closed squares-amphibolites and diamonds-breccia clasts. from Floyd and Winchester, 1977).

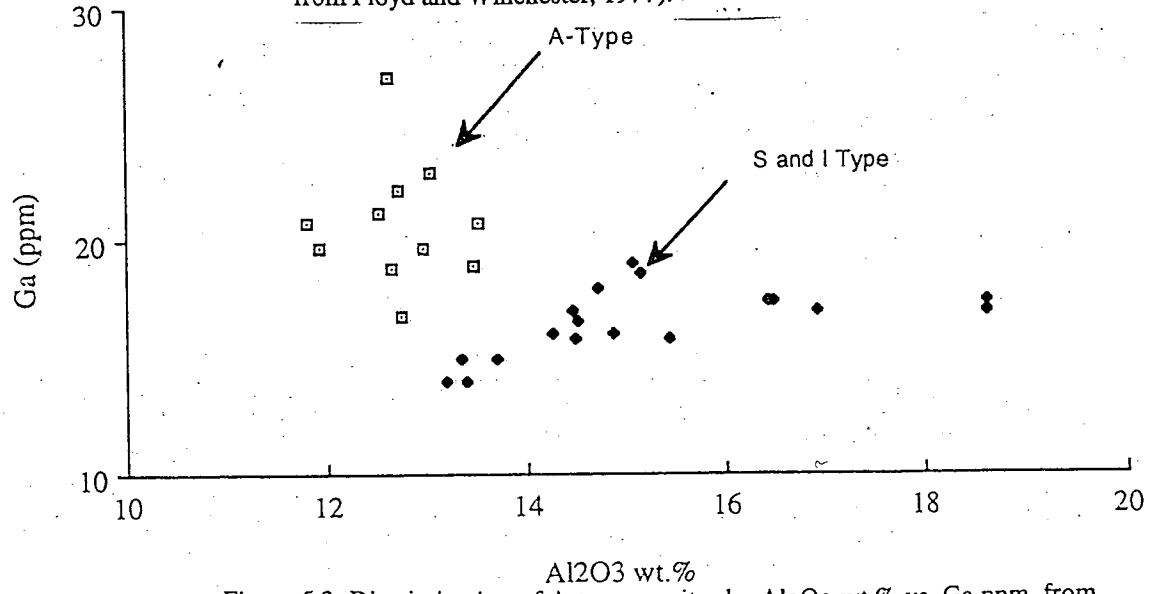

Figure 5.2 Discrimination of A-type granites by Al_2O_3 wt.% vs. Ga ppm, from Collins et al. 1982.(open squares -Pt. Victoria rhyodacites and diamonds I and S type data from Chappel & White, 1992 and Chappel, 1989).

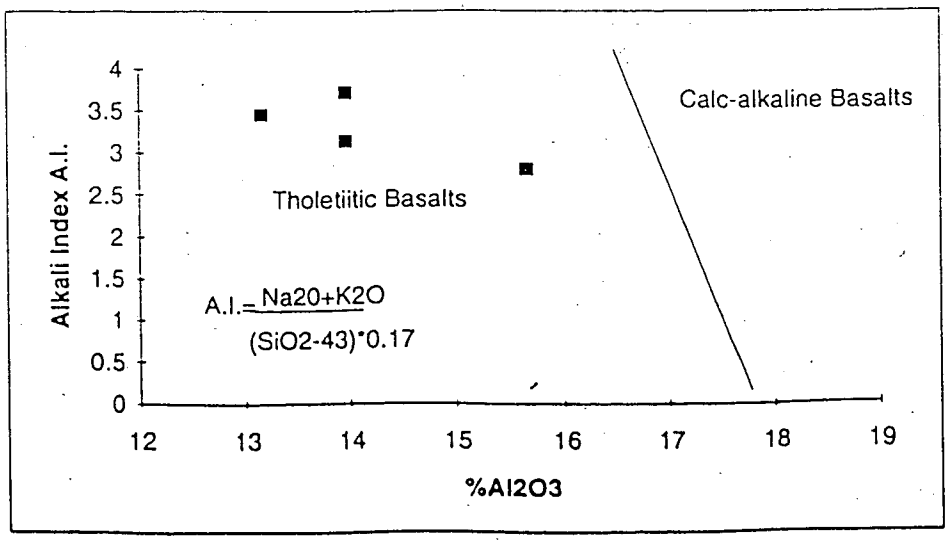

Figure 5.3 Discrimination of tholeiitic basalts using A.I. vs. Al2O3 wt. % (from Wilson, 1987).

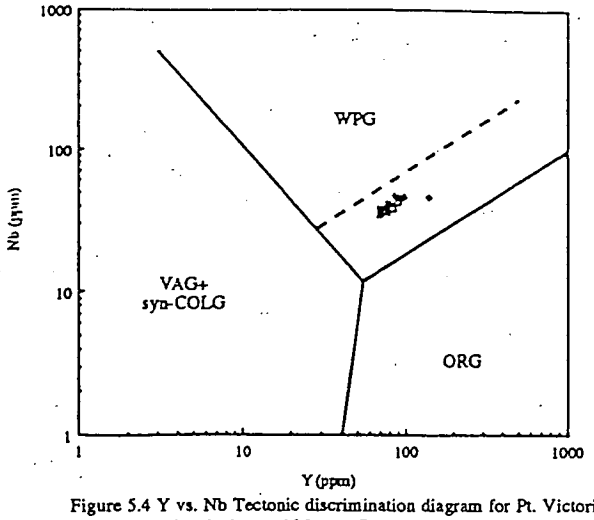

Figure 5.4 Y vs. Nb Tectonic discrimination diagram for Pt. Victoria rhyodacites and Moonta Porphyry. (WPG = within plate granites & dashed line is upper boundary of ocean ridge granites).

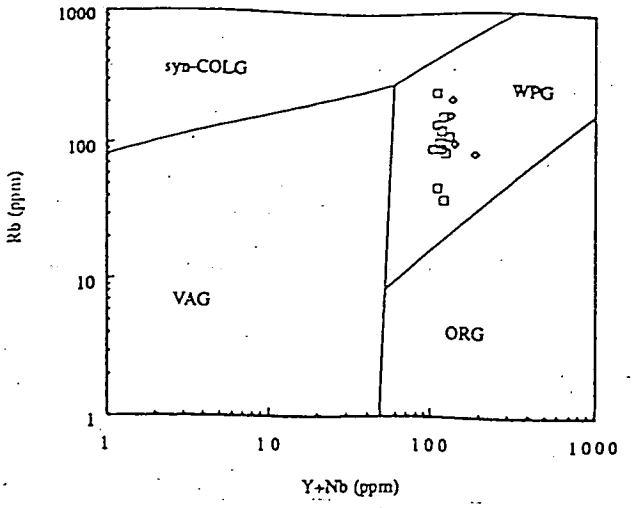

Figure 5.5 Y+Nb vs Rb Tectonic discrimination diagram for Pt. Victoria rhyodacites and Moonta Porphyry.

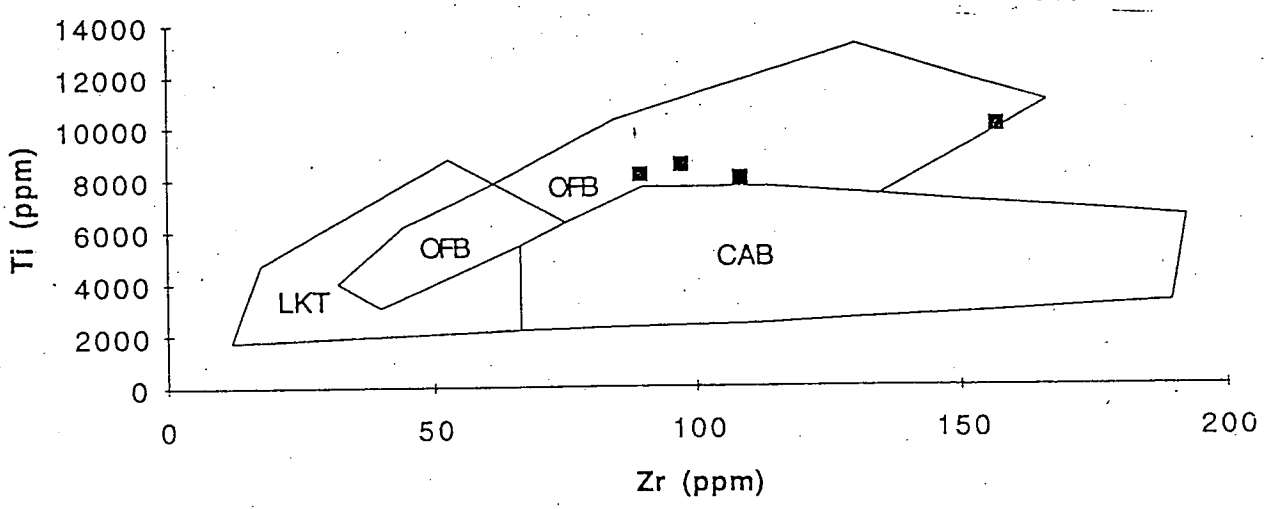

Figure 5.6 Tectonic discrimination diagram for basic rocks. OFB- ocean floor basalts, CAB- calc-alkali basalts and LKT- low pottasium basalts (after Pearce & Cann, 1974).

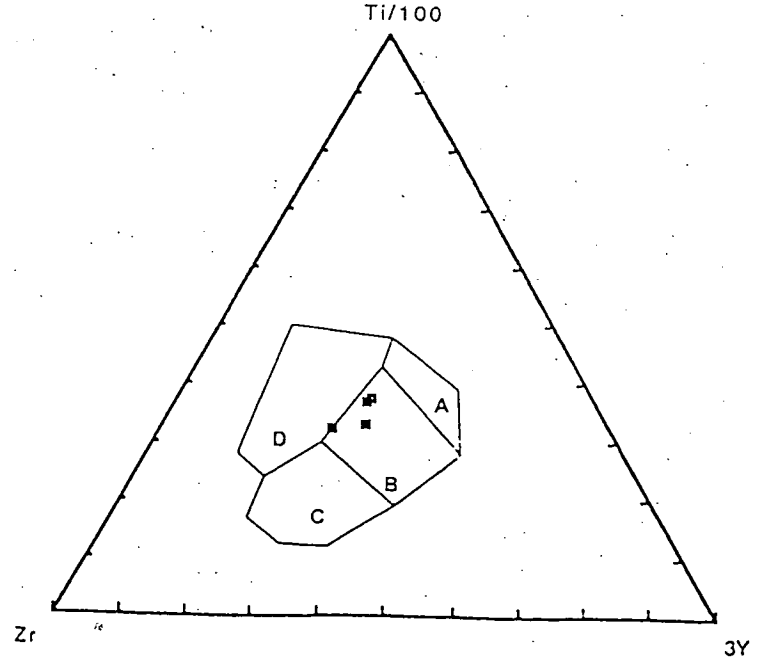

Figure 5.7 Ti/100, Y.3 and Zr tectonic discrimination diagram for basic rocks. A &B- low pottassium tholeiites, B- ocean floor basalts C & B- calc-alkali basalts and D- within plate basalts

Chapter 6. Comparative Geochemistry

6.1 Introduction

Wyborn et al. (1992) have divided Proterozoic felsic magmatism in Australia, into five main groups; 1) I-type, Sr-depleted, Y-undepleted, restite-dominated granites; 2) I-type, Sr-depleted, Y-undepleted, fractionated granites, low in incompatible elements; 3) I-type, Sr-depleted, Y-undepleted, enriched in incompatible elements (anorogenic granites); 4) I-type, Sr-undepleted, Y-undepleted and 5) S-type granites, Sr-depleted, Y-undepleted. The Pt Victoria rhyodacites fall into the third of these groups which includes a number of South Australian examples, represented by the Moonta porphyry, McGregor, Gawler Range and Tidnamurkana volcanics. In the following chapter the Pt. Victoria rhyodacites were compared with these on multi element variation diagrams (Sun and McDonough, 1989). In addition to these Proterozoic volcanics, comparisons included the Bosanquet and Nuyts volcanics which represent Early and Late Proterozoic volcanic units from the Gawler craton.The reason for their inclusion was to establish if there were any patterns of source evolution in the Proterozoic. Another reason for this comparison was to determine if the volcanics at Pt. Victoria have any affinities with other units in the region. Comparisons of the basic rocks from Pt. Victoria with other basic units were made for the same purpose.

6.2 Felsic volcanics

The Pt. Victoria rhyodacites were compared with a number of above mentioned South Australian volcanics to determine if any relationship existed. It should be noted that Wyborn et al (1987) identify a suite 1810-1620 Ma which are all anorogenic and all units apart from the Bosanquet (~1845 Ma) and the Gawler Range Volcanics (GRV ~1592 Ma) are contained within this suite. When all the volcanics are plotted on a multi element variation diagram they show a broadly similar pattern with the exception of the Bosanquet which supports Wyborns classification. The Pt. Victoria samples can be seen in Figure 6.1 to most closely resemble the Moonta Porphyry and the Tidnamurkana volcanics, showing similar element values across the range with the exception of Pb, Sr and P. The McGregor volcanics erupted at a similar time (1766 Ma U-Pb) were also compared (Figure 6.2) but show a difference in the incompatible and rare earth elements Y, Nb and La. To establish if a spatial relationship existed the Bosanquet, McGregor and GRV all located on northern Eyre Peninsula were compared (Figure 6.3). The Mcgregor and GRV have similar patterns and values for many elements. The Bosanquet however are older and part of a suite identified by Wyborn et al. as forming from crustal sources, unlike the others which are anorogenic. A final comparison was made between the Bosanquet, Pt. Victoria and Gawler Range Volcanics to determine if any temporal evolutionary pattern existed (Figure 6.4). Elements such as Y, Zr and Nb do show an age progression but on the whole the element composition does not show decreasing values with age.

Any evaluation of the comparisons must consider that the processes leading to felsic products are varied, partial melting, fractionation etc., while basaltic rocks are more likely to represent a primary composition. This is to say that while two volcanics have a common source, different evolutionary processes can be reflected by varying elemental compositions. There are some obvious similarities such as the Pt. Victoria, Moonta Porphyry and Tidnamurkana volcanics indicating a common source, but the differences of the McGregor volcanics of a similar age is conflicting. The differences between the spatially related Bosanquet, Mcgregor and GRV also seems to reflect this. However on the basis of the anorogenic nature of the Proterozoic rocks compared some similar source characteristic must have existed. This may be indicative of an enriched mantle source. The fact that no temporal evolution can be seen suggests depletion of a homogenous source was not prevalent, but a variably enriched mantle source existed.

6.3 Basic Rocks

The amphibolites from Pt. Victoria were compared with a number of basic units of different ages from bimodal, basic-intermediate-acid and solely basic associations. The amphibolites were plotted on primitive mantle normalised multi-element variation diagrams. The units compared were the adjacent Wardang Island and Adelaidean Adelaide geosyncline basalts (Figure 6.5a). Basalts from the West Australian Archean Welcome Well and Proterozoic central Australian provinces (Figure 6.5b) and two basalts from the Gawler Range Volcanics (GRV) province, the Nuckulla and Kokatha basalts (Figure 6.5c) were also included.

Figures 6.5 a-c show that obvious differences and similarities exist. Figure 6.5a shows that the Wardang Island and Adelaide Geosyncline basalts have similar patterns, with the exception of the elements Ba and K which are more mobile. This could result from a similarity in the source region. The West Australian Welcome Well Archean complex has both higher and lower values for many incompatible elements, while the Proterozoic central Australian province is consistently higher across the range of element (Figure 6.5b). This highlights the differences in a temporal and spatial sense, whilst a common source is not evident on the basis of the data. This difference in source is further supported by Figure 6.5c where the GRV units have higher values, with the exception of Ti and Y. If a common source is invoked, continous depletion of this source as a result of prior events would be expected. The fact that this is not the case is demonstrated when the felsic associations of these Proterozioic areas are compared at the same SiO_2 contents as the Pt. Victoria rhyodacites. The incompatible elements are equivalent or greater which suggests an enriched mantle source existed in the Proterozoic which was not homogenous, but variable.

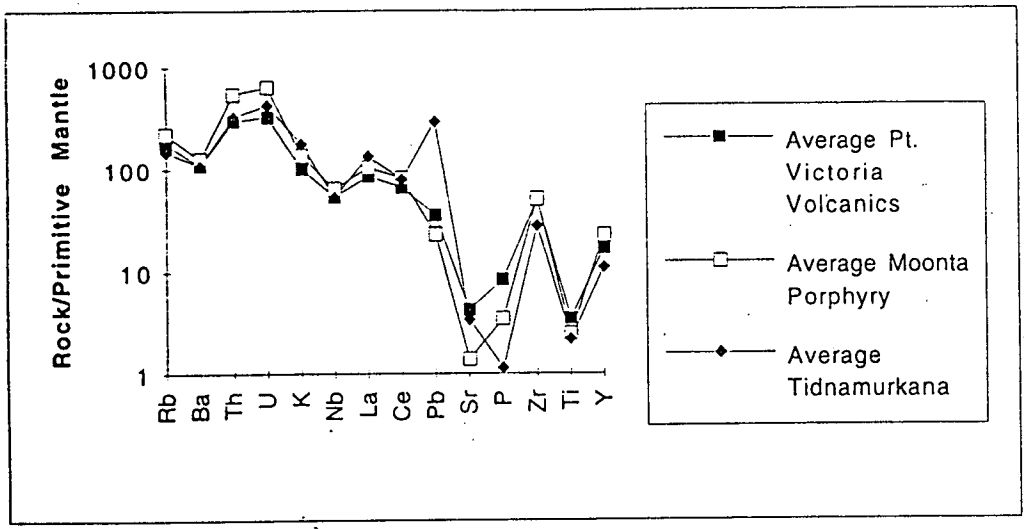

Figure 6.1 Comparisons of Pt. Victoria, Moonta Porphyry and Tidnamurkana Volcanics

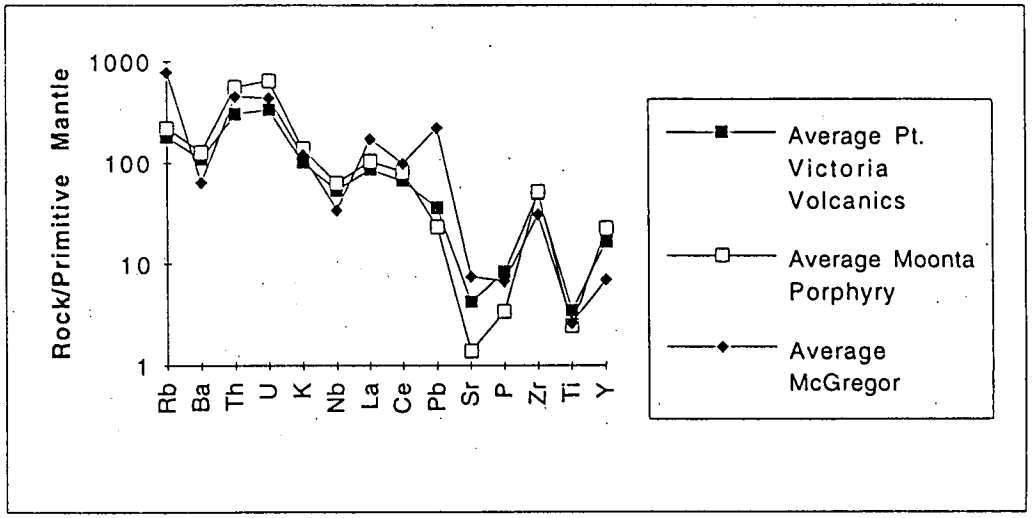

Figure 6.2 Comparison between the Pt. Victoria, Moonta Porphyry and McGregor Volcanics

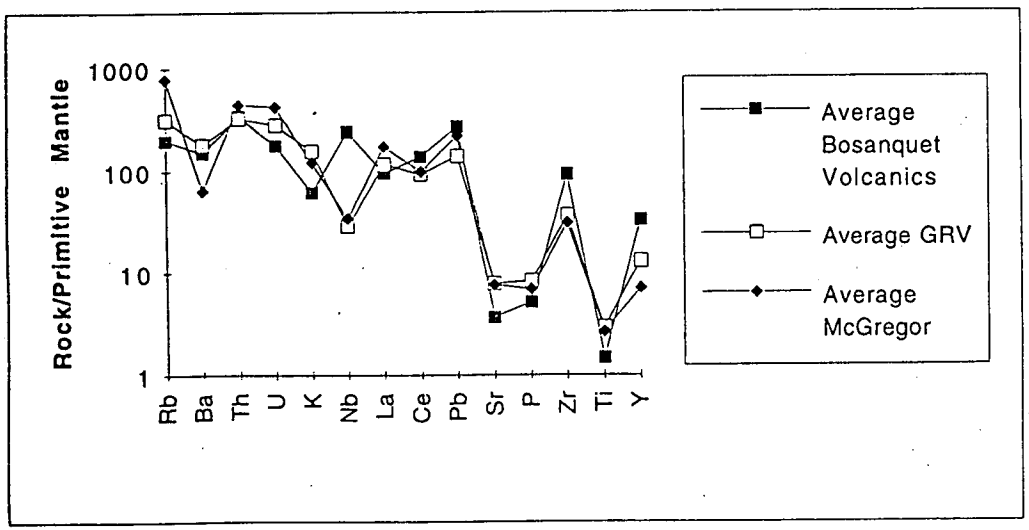

Figure 6.3 Comparison between the Bosanquet, McGregor and Gawler Range Volcanics

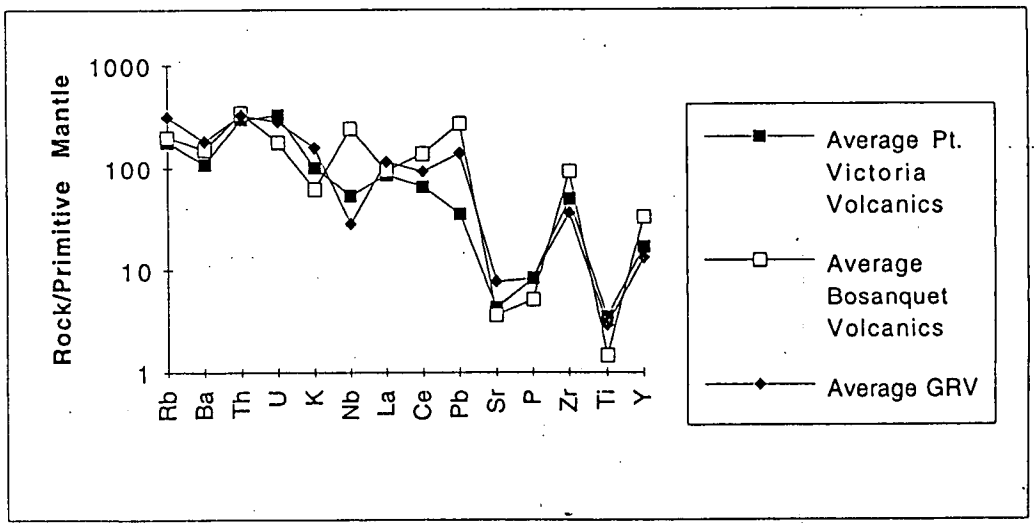

Figure 6.4 Comparison between the Pt. Victoria, Bosanquet and Gawler range Volcanics
(GRV data from Stewart, 1992; Bosanquet, Tidnamurkana and McGregor from SADME)

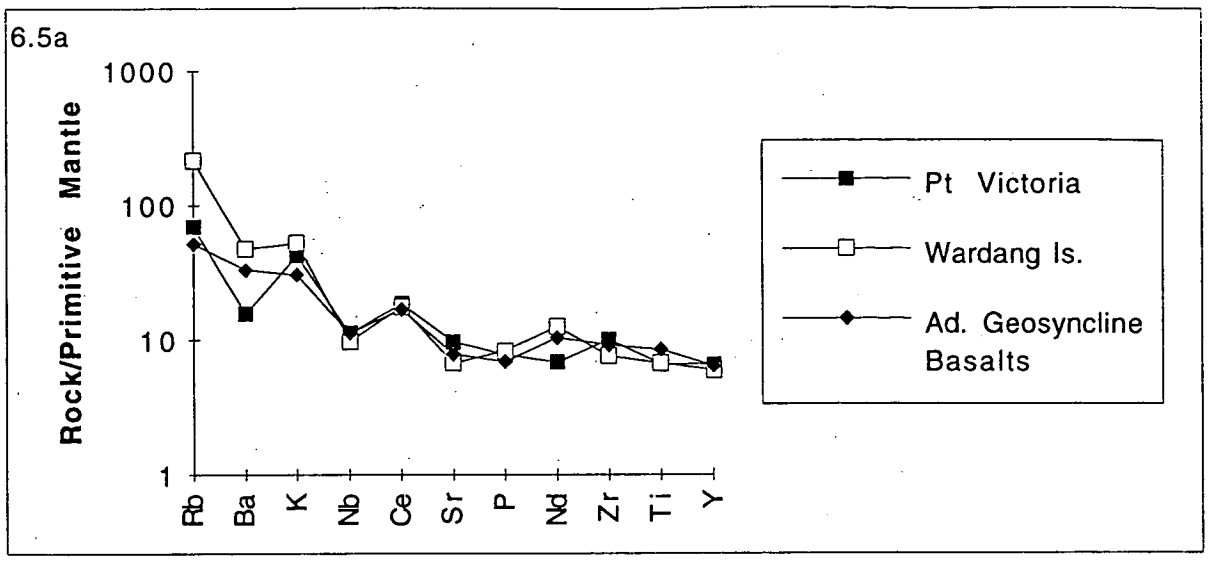

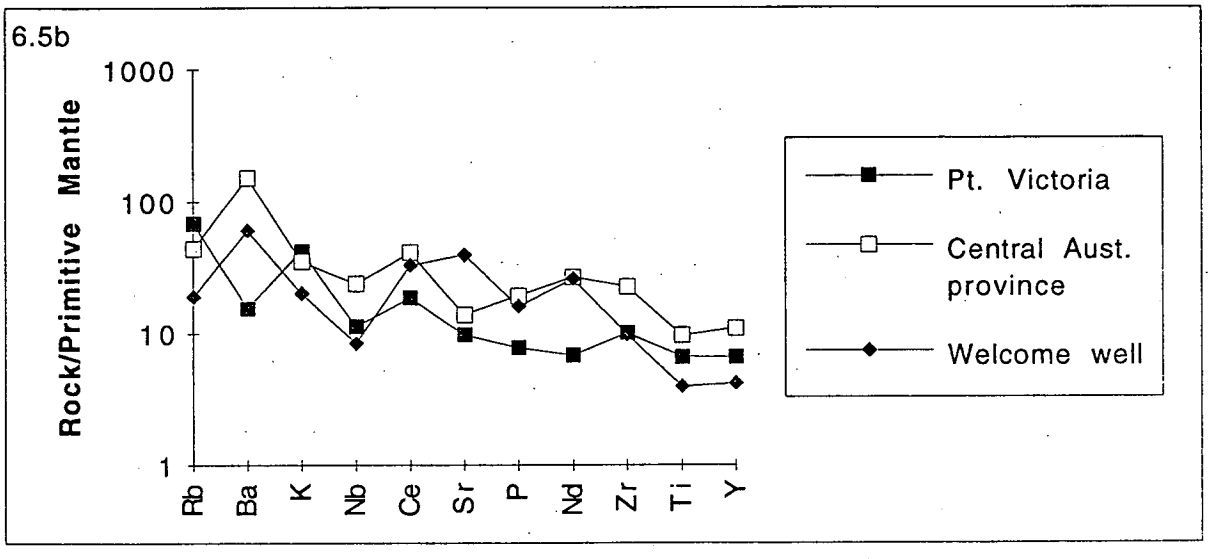

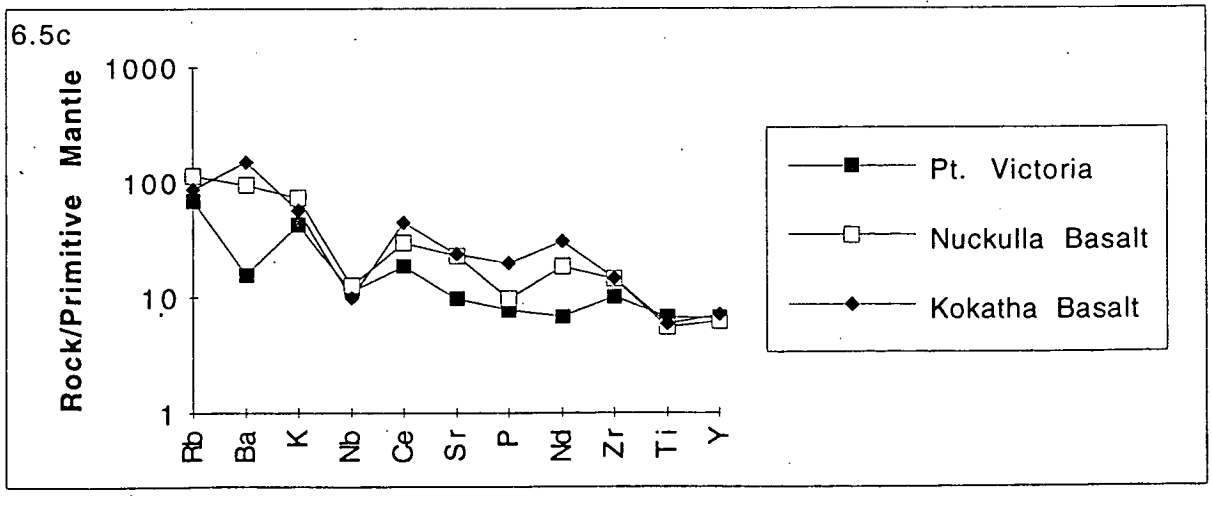

Figures 6.5 a-c Multi-element variation diagrams comparing the Pt. Victoria amphibolites with various other Basic suites.(see text for explanation, Adelaide Geosyncline Basalts data from Giles Teale, 1976 and others Giles, 1980).

Chapter 7. Isotope Geology & Geochronology

Introduction

Rb/Sr and Sm/Nd isotopic analysis was carried out to establish a geochronological framework for the rocks at Pt. Victoria. In addition it can provide information on the petrogenesis and source of the of the lithologies. 8 samples were analysed for the isotope systems mentioned above with 6 whole rock and 2 mineral separates . For a full description of the analytical techniques the reader is referred to Appendix 3. The samples analysed are one amphibolite and rhyodacite, 4 adjacent layers from the layered metasedimentary unit and biotite and muscovite mineral separates from the massive metasediment. Mineral separates are useful in that they are sensitive to lower temperature changes because closure temperatures are much lower for minerals than whole rock samples. For a summary of the isotopic parameters used and relevant equations see Appendix 4.

7.1 Rubidium-Strontium Systematics

The basis of Rb/Sr geochronology is the radioactive decay of ^{87}Rb to ^{87}Sr which over time cause changes to the $^{87}Sr/^{86}Sr$ ratio. An example is when a magma crystallises all rocks produced will have the same initial $^{87}Sr/^{86}Sr$ ratio. When plotted on a graph with the the axes (x) $^{87}Rb/^{87}Sr$ and (y) $^{87}Sr/^{86}Sr$ all samples from such a suite create a straight line called an isochron. The slope of this line defines an age which is basically the time past since all the rocks had the same initial $^{87}Sr/^{86}Sr$ ratio and have remained a closed system. Increases in ambient temperature such as metamorphism can cause a system to become open resetting the $^{87}Sr/^{86}Sr$ ratio (Faure, 1977).The result of this is that these samples will plot further away from an isochron representing the crystallisation age of the sampled rocks and define a new isochron (Fanning, 1985).

Bone (1978,1984) carried out Rb-Sr whole rock analysis on the rhyodacites from Wardang Island. The results of this yielded a variety of ages but the removal of dubious outliers returned an age of 1734±42 Ma. The results of this analysis are seen in Table 1 with the analyses from Pt. Victoria. The inital ratio of Bone's data was 0.698 which is lower than that considered to have existed in the primitive mantle. On this basis Fanning (1985) considers that the system has been open at some time in the past altering the systematics. Bone's data was plotted with the whole rock data from Pt. Victoria with the resulting isochrons, one fitted to the whole data set and the other to Bones data alone seen in Figure 7.1. The age produced using the combined data was 1592 Ma and all of Bone's data produced 1766Ma .

The data from Pt Victoria was plotted producing a number of isochrons using the slope of the best fitted line to calculate the age, with the exception of the four metasediments which were also calculated using the least squares method. The first of these was a four point isochron using four adjacent layers of the metasediment (Figure 7.2). This was to determine if a

metamorphic event had occurred. If it had, isotopic homogenisation would be expected and the adjacent layers would behave as a unique system. Unmetamorphosed the layers are compositionally different and likely to have differing Rb-Sr values which when plotted would be unlikely to define a good isochron. When calculated the four layers had an age of 1513 Ma with an initial $^{87}Sr/^{86}Sr$ ratio of .71997. This was also calculated using the method of least squares regression of McIntyre (1966) and when regressed had an age of 1507±105 Ma, with an MSWD of 1. A second whole rock isochron (Figure 7.3) was regressed using the amphibolite and rhyodacite samples in addition, this provided a six point isochron which is expected to be more accurate as it contains more points. This yielded an age of 1540 Ma with an initial ratio of 0.71570. The similarity between these two ages indicates a metamorphic event strong enough to reset the whole rock systematics.

Evidence for such an thermal event in a regional context is provided by Webb et al. (1986) who have dated pegmatites from the Moonta suite at 1400-1500 Ma by Rb-Sr methods. The presence of similar pegmatites in the Pt. Victoria area may be associated with this event. Bone (1978) plotted a number of regressions with one of the better fitted isochrons achieved using 9 samples from the north west and west coast producing an age of *ca* 1420 Ma and initial ratio .723. This is also in keeping with the whole rock data from Pt. Victoria and the Moonta pegmatites. The Arthurton granite dated at 1585±3 Ma by U-Pb may also provide the heat source for the resetting event indicated by whole rock data from Pt. Victoria.

The above isochrons were plotted using Rb-Sr values obtained from whole rock analyses the next two were done so using mineral separates. The first of these is a seven point isochron using the muscovite and whole rock values (Figure 7.4) and returns an age of 1296 Ma with an initial ratio of 0.73374. Webb op cit. have dated two granites from the Moonta area, the first is from a granite from a drill hole South of Moonta and gives a Rb-Sr age of 1282±179 Ma. The other is from the Tickera Granite and gives a Rb-Sr age of 1215±554 Ma. These may have produced a temperature which was able to reset the system in the mineral separates but not the whole rock.

The biotite was also regressed with the metasediments and lies much further away from the others with a $^{87}Rb/^{86}Sr$ of 1177. It returns an age of 481 Ma which is very young for the area considering it was stabilised at approximately 1400 Ma and the youngest event following this was the intrusion of the post orogenic Tickera granite. Cliff (1985) has stated that biotite remains open to Rb-Sr after other minerals have ceased to do so, however it is not realistic that it would stay open for a further 800 Ma. The date of 481 Ma is within the realms of the last activity of the Delamerian orogeny from the adjacent Adelaide fold belt which occurred in the time range of 515-485 Ma.The proximity of Pt. Victoria to the hinge zone may provide the only explanation in the form of a late stage thermal pulse from this region.

7.2 Neodymium-Samarium Systematics

The REE Sm and Nd are useful tools for geochronology because they are not as easily mobilised as the alkali metals rubidium and strontium considered previously. As a result of this they can be used to establish primary ages in systems which have not been closed to Rb-Sr (Faure, 1977). Model ages can be calculated from these, which in its simplest form represents the time at which a particular piece of crust separated from the mantle. McCulloch (1987) recognises that since the method of dating by Sm-Nd was developed on the basis of CHUR (chondritic uniform reservoir), which had its Sm-Nd composition estimated from meteorites advances have been made. It has been refined to encompass a more complex depleted mantle evolution as a reference and model ages calculated from this which will be referred to unless otherwise stated.

The metasediments display εNd values at present of between -24 and -26 which are all similar and so sourced from a similar parent assuming that the systematics have not been disturbed. The metasediments have lower $^{143}Nd/^{144}Nd$ ratios than the amphibolite and rhyodacite (see Table 1). This indicates that they are older than the intrusives as the $^{143}Nd/^{144}Nd$ ratio has been evolving with time from the initial CHUR ratio. Three of the samples, 13a-c have depleted mantle model ages (T_{DM}) in the range 2.34-2.56 Ga while 13d differs greatly at 3.95 Ga. Nevertheless this indicates an Archean source for the sediments supported by Figure 7.5 which shows the evolution of εNd with time including the Archean source field of Turner et al., 1993. Further support for these having an Archean source is additional data from Turner op cit. who analysed a number of samples from the Gawler Craton basement including mafic granulites, felsic gneisses, paragneisses and unmetamorphosed rhyolites. These have εNd values at their model ages of between +4.2 and -6.32 with the metasediments having values of +2.25 and so occurring within this range. The T_{DM} as seen above are close to those of Turner op cit. at 2.6-4.1 Ga.

The rhyodacite has an epsilon Nd at present of approximately -15, and a depleted mantle model age of 2.09 Ga which supports them being younger than the sediments as seen in figure 7.5. The εNd value at 1740 their assumed age of crystallisation is 0.88. This is a positive value which would indicate a mantle source with a minor crustal component.This is also supported by figure 7.5 which shows that the rhyodacites are isotopically primitive evidenced by the short period between extraction and extrusion at 1740 Ma (pers. comm. J. Foden, 1993). Early to Middle Proterozoic basement from the Gawler Craton was also sampled by Turner op cit.. The rhyodacites equate most closely to the Mid-Proterozoic units of the McGregor and Gawler Range Volcanics, which also included the Corunna Conglomerate. These have εNd ranges from +1.2 to -3.8 and a T_{DM} of 2.0-2.5 which compares favourably to the Pt Victoria rhyodacite.

The rhyodacite was considered as a possibility for the enigmatic source of the Adelaidean sediments in the adjacent fold belt. The T_{DM} of the rhyodacite lies within the range of 1.8 to 2.2 Ga and even closer to the mean of 1.9 from Adelaidean sediments analysed by Turner op cit. The εNd of the rhyodacites calculated at 700 and 800 Ma were -8.73 and -7.81 respectively and are similar to the Callana Group εNd -8.8 and the Umberatana -8.5. Therefore on the basis of εNd data a tentative correlation may be drawn, however more extensive petrological comparisons would be required.

The amphibolite presents more of a problem, with a present $^{143}Nd/^{144}$ ratio of .512052± and an unrealistic model age of 84 Ga. This could be accounted for by the fact that the amphibolite may have evolved on a path which is nearly parallel to that of the depleted mantle. As a result of this the point where it intersects the evolutionary path of the depleted mantle, where the model age is taken from is out of the time scale of the earth (Figure 7.6) (pers. comm J. Foden, 1993). The fact that it also has a high negative εNd value at 1740 Ma could also support this assumption since the depleted mantle unlike CHUR evolves to progressively more negative εNd values.

	Rb ppm	Sr ppm	Rb/Sr	87Sr/86Sr	87Rb/86Sr
Sample No.					
Whole Rock					
1002-13a	114.4	101.4	1.1283	0.78887	3.2905
1002-13b	509.4	131.3	3.8782	0.9689	11.5073
1002-13c	30.3	90.6	0.3347	0.74292	0.9718
1002-13d	452.1	127.2	3.552	0.95034	10.5209
1002-35	111.3	220.6	0.5043	0.74209	1.4639
1002-70	119.4	65.6	1.8914	0.83255	5.3282
Mineral Separates					
1002-31Bt	280.9	18.1	15.4493	8.89038	48.7365
1002-31MsB	834.8	3.6	226.0229	1.63108	1177.415
Wardang Is. Bone,1978					
524-601	184	72.8		0.885	7.4278
524-602	224	92.3		0.87805	7.1494
524-604	214	82.1		0.89489	7.7207
524-605	217	81.3		0.898	7.8738
524-606	216	81.3		0.89485	7.8269
524-607	198	97.2		0.84513	5.9889
524-611	181	93.1		0.83913	5.7163
524-613	204	120		0.82472	4.9587
524-614	198	121		0.82067	4.769
524-615	192	115		0.82164	4.8748

	Nd ppm	Sm ppm	Sm/Nd	143Nd/144Nd	147Sm/144Nd	
Sample No.						
Whole Rock						
1002-13a	29.6	5.6	0.189	0.51138	0.1143	-6.2
1002-13b	25.7	4.6	0.1816	0.51132	0.1099	-6.4
1002-13c	42.05	7.1	0.1711	0.51138	0.1035	-3.8.
1002-13d	15.8	3.8	0.2407	0.5113	0.1456	-14.8.
1002-35	19.9	7.05	0.3542	0.51205	0.2143	-15.5
1002-70	54.8	11.3	0.2066	0.51186	0.125	0-8 1.

m/ seds south of the jetty.
Amphibolite (nth of jetty)
Rhyodacite ? sth of jetty.

Table 1 Nd-Sm and Rb-Sr Isotopic Results summary

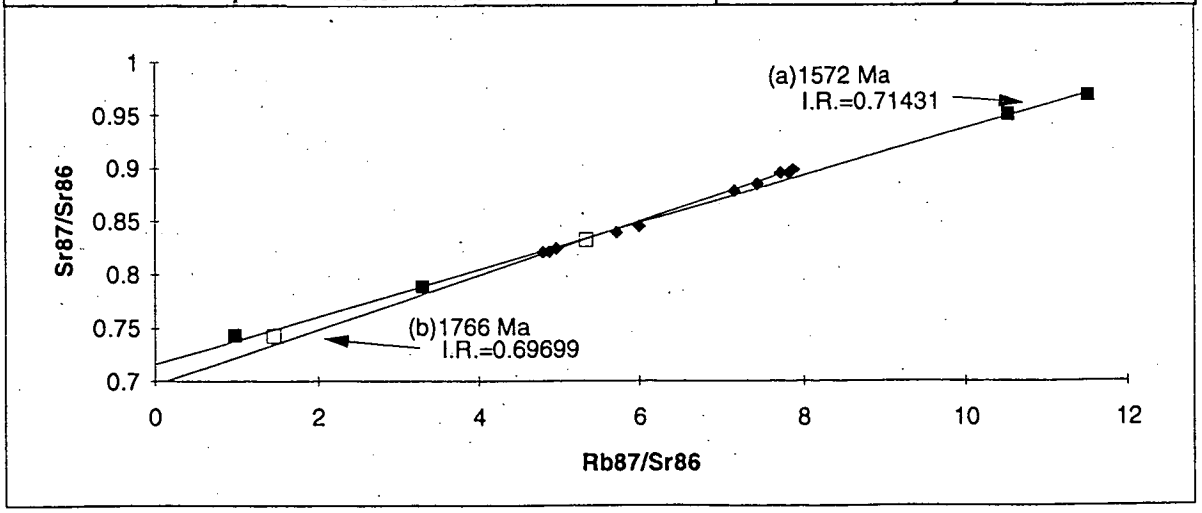

Figure 7.1 Whole rock isochrons showing a) Pt. Victoria data combined with Bones data and b) Bones data alone.

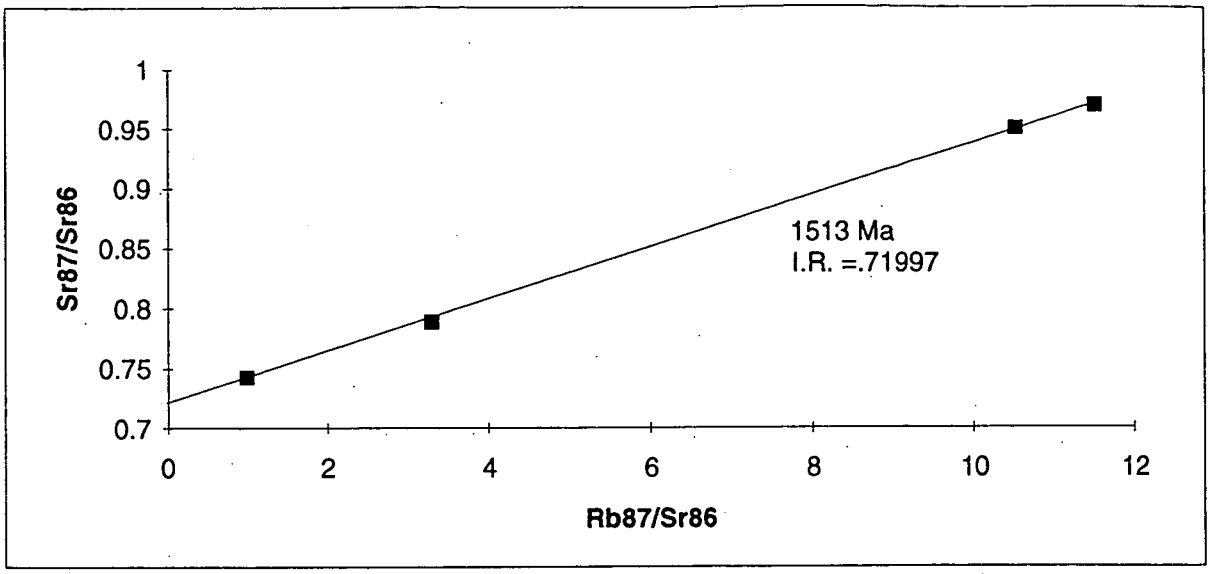

Figure 7.2 4 point Whole rock isochron using metasediment interlayers

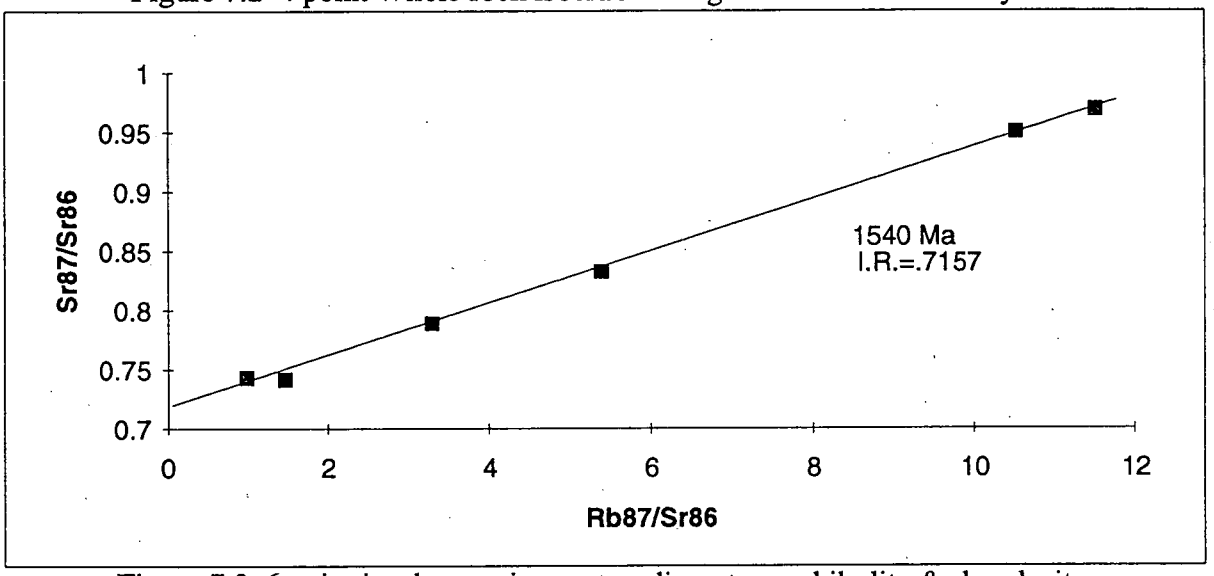

Figure 7.3 6 point isochron using metasediments,amphibolite & rhyodacite

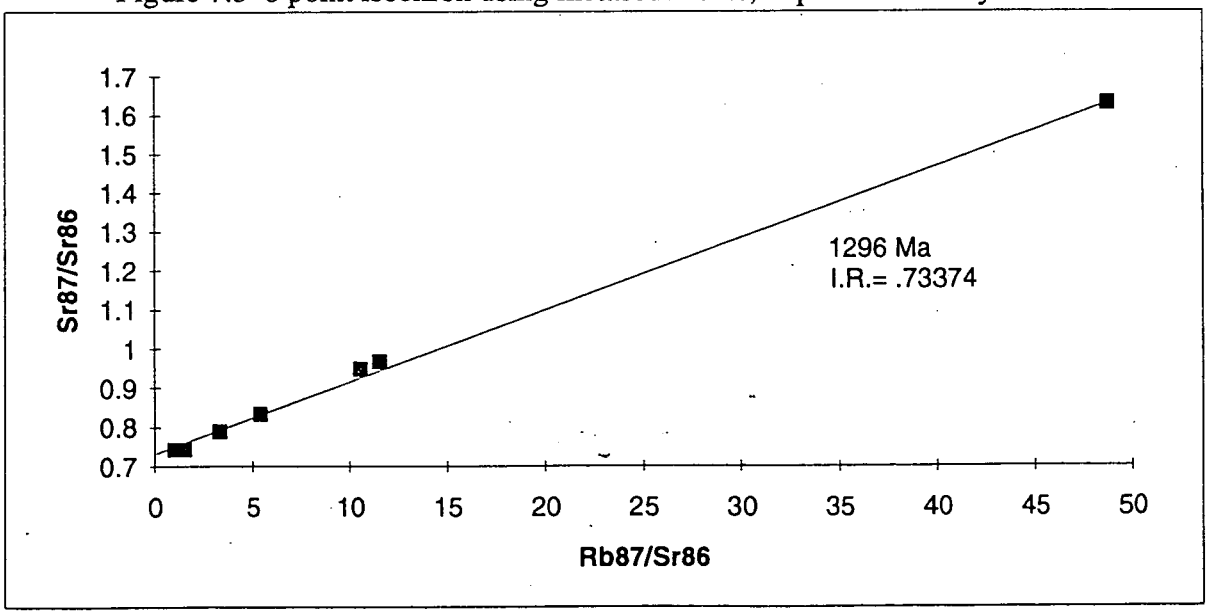

Figure 7.4 isochron using whole rock data and muscovite mineral separate

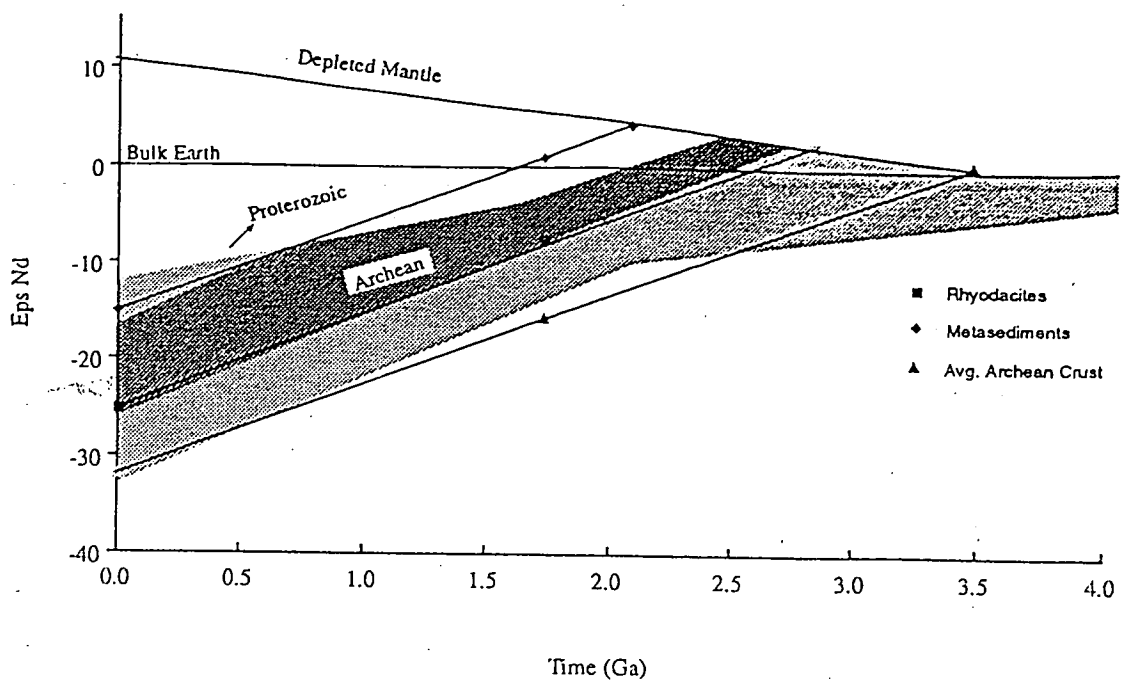

Figure 7.5 Epsilon Nd vs. Time showing evolution of Epsilon for Metasediments, Rhyodacites and average Archean crust, with Archean and Proterozoic source field of Turner et al., (1992).

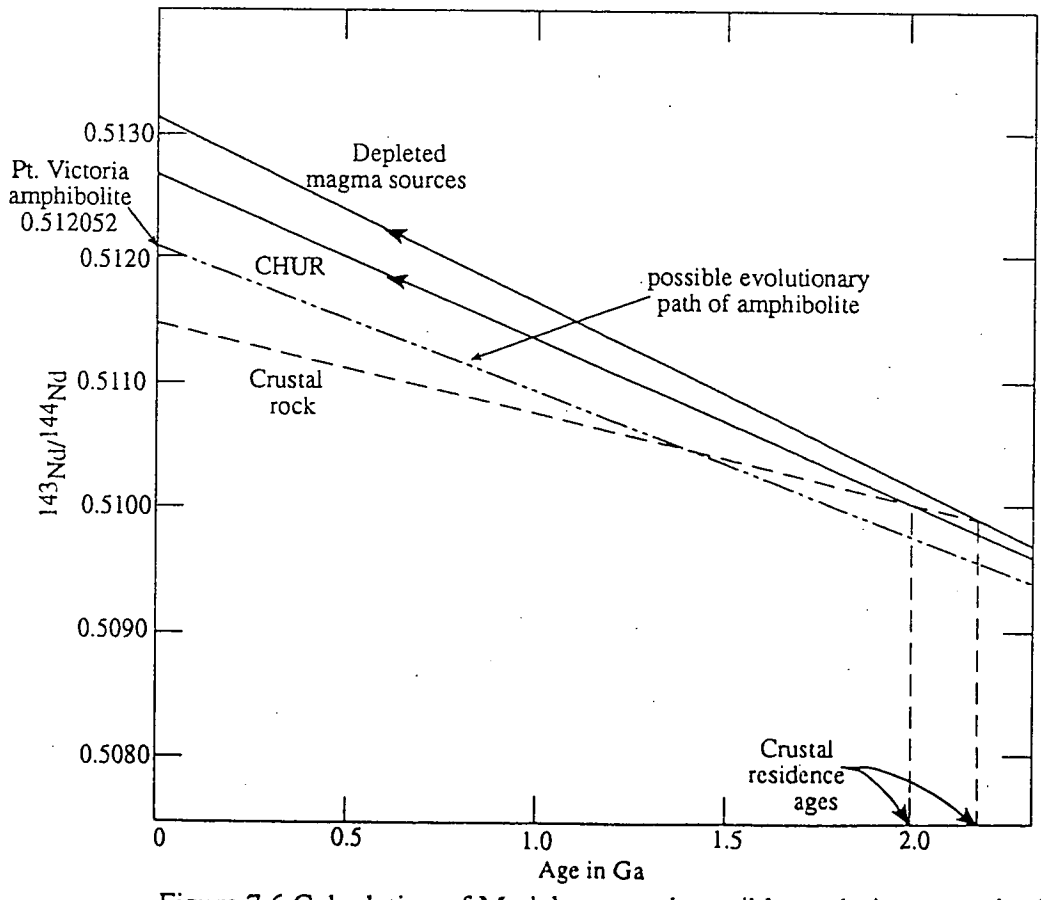

Figure 7.6 Calculation of Model ages and possible evolutionary path of amphibolite (after Faure,1977).

Chapter 8. Petrogenesis

The volcanic suite at Pt. Victoria is represented by basic intrusives, intermediate porphyritic breccias and the dominant rhyodacite which is the focus of this section. These rocks are considered to fall within the 1810-1620 felsic suite of Wyborn et al. 1987 and are related to the Moonta porphyry. The felsic rocks of this period have $SiO_2 > 68\%$, are enriched in incompatible elements are anorogenic and have a red colouration in hand specimen. The granitic rocks from the period 1740-1620 are often associated with basic complexes imparting a bimodality which will be considered (Wyborn et al., 1987). The source of Proterozoic granites is not known as most are Sr depleted and Y undepleted, the opposite is seen in the Archean rocks which are ruled out as a possible source because they are Y depleted. Subduction as we know it today is also considered not to have occurred. It is however believed that the Proterozoic was a period of extensive crustal generation but a source has still yet to be definitively identified (Wyborn et al. 1992). The rhyodacites have been identified as A-type in character and a number of theories have been forwarded to account for their petrogenesis.

The problem in assessing the rocks of the study area with the proposed models of petrogenesis is that although compositionally similar they are based on plutonic rocks not from the Proterozoic. When the suite of rocks are plotted on simple variation diagrams of various major and trace elements versus SiO_2 (Figures 8.1 and 8.2), some elements in the cases of MgO and TiO_2 do equate to what could be called a liquid line of descent. This is where a coherent trend in terms of the evolution from a more basic rock through to a more SiO_2 rich differentiated product is seen. However as seen the above examples are more the exception than the rule, with the bulk of variation plots showing much less coherence and indicating in most examples a distinct bimodality. As mentioned in the introduction this bimodal character is not unusual for this period, and could be accounted for by the fact that rocks of intermediate composition are not common in the Proterozoic (McCulloch, 1987). This does not discount fractionation as a possible factor, but negates the affinity of the breccia to the rhyodacite with the major and trace elements being much higher in the breccia at lower SiO_2 contents. Thus it is unlikely that the rhyodacite is the product of fractionation of the breccia which represents a unique component in the system.

Fractionation however has been considered as a possible mechanism for the generation of A-type granites. Whalen et al. (1987) note that many A-type suites consist of large proportions of felsic rocks which in plutons do not show large amounts of internal differentiation or intermediate counterparts. Fractionation is seen as variations in the Rb/Sr and Rb/Ba ratios. There is some variation in these values observed in the Pt. Victoria suite, however these variations when ranked in order of increasing SiO_2 across the range do not show a progression. The variation is likely the result of mobility of Sr and Ba. On the other hand Creaser et al. (1991) notes that the suggestion has been made that granites which have < 70 ppm Sr have experienced crystal fractionation. A third of the samples show < 70 ppm Sr with

the majority above this, however the nature of the system may be such that Sr has been mobile. The trough in the Sr values seen in the multi element variation diagrams from section 6 for Pt Victoria could account for fractionation. Wilson (1987) notes that such a trough is the result of feldspar fractionation from basalts. Whalen et al. consider that fractionation as the sole process would not be able to account for the observed chemistry which characterises A-type granites. Emphasis should be placed on the fact that it is not able to produce these compositions on its own. The geochemical evidence indicated above would seem to support the fact that fractionation has played a role in the evolution of the rhyodacites. This will be elaborated on in a consideration of the process of assimilation and fractional crystallisation (AFC).

Partial melting has been proposed by Whalen et al. (1987) and Creaser et al. (1991) as a means of A-type generation. Collins et al. (1982) propose that the genesis results from the remelting of a residual source which has already given rise to a partial melt on the basis that anorogenic granites being late stage events would have a source which had produced a melt for magmas produced prior to this. The characteristics of A-type magmas are also explained in terms of a residual source. However in a more recent assessment Creaser et al. believe that the major element chemistry is not consistent with the production of unfractionated magmas from a residual source (Creaser et al., 1991). Both Creaser and Whalen consider that a granulite facies residual source is not necessary to generate the anhydrous melt required for the formation of an A-type magma. One suggestion is that halogen rich volatiles derived from the mantle flux into the system and generate melts as well as providing the source for the alkalis and enrichment in incompatible elements (Whalen et al., 1987). However both consider that the necessary conditions and compositions can be achieved by the partial melting of a lower crustal meta-igneous source of tonalitic to granodioritic composition and need not have experienced granulite facies metamorphism. The anhydrous nature of the subsequent melt arises from the vapour absent breakdown of hydrous minerals in the source which generates the volatiles needed to drive partial melting and provide the incompatible elements. The magmas are F and Cl rich and would provide the sites for the high field strength elements (HFSE) in response to the disruption of the framework of aluminosilicates (Whalen et al., 1987 and Creaser et al., 1991).

As mentioned in section 5 the temperatures associated with A-types melts are high and these are produced by the intrusion of mantle derived mafic material in the lower crust. Wilson (1987) notes that the Sm/Nd ratio is fractionated, as is the Rb/Sr by the process of partial melting. As a result partial melts display a lower Sm/Nd ratio but a greater Rb/Sr than the mantle derived materials from which they were sourced. This relationship is displayed between the rhyodacites and amphibolites which would be considered the mantle derived component. The Sm/Nd of the rhyodacite and the amphibolite are 0.2066 and 0.3542 respectively, and the Rb/Sr is 1.8914 and 0.5043 thus meeting the above criteria. This provides some evidence for this process which has been the dominant feature of recent literature.

Another possibility which expands upon the initial idea of fractionation, is the process of assimilation and fractional crystallisation (AFC). This could occur in a high level magma chamber which is common in volcanic areas. The system would also be closed accounting for the observed lack of intermediate outcrop in the field. The process of AFC can be developed in conjunction with a model of the development of such a system. Huppert and Sparks (1988) propose a model involving the injection of basaltic magma into the crust in response to a tectonic process such as extension or mantle pluming. Both are believed to have been dominant in the Proterozoic, notably pluming in terms of ensialic rifting as proposed by Wyborn (1988). During this initial period of intrusion the heat has not propagated through the crust and so a near normal geothermal gradient still prevails. The implications of this are that the temperatures required for crustal melting are not reached and some of the intrusive material may reach the surface. This could be represented by the mafic-intermediate breccia which is considered to have been extruded before the felsic rocks. Although no isotope data is a available its major and trace element composition separates it from the rhyodacite. The idea of a heterogeneous mantle created by re-enrichment of zones of the mantle by metasomatism is considered to occur. If for example a plume was responsible for the initiation of the process of intrusion, the rising body of depleted mantle material may pass through such an enriched zone and cause it to rise at the margins of the plume. It may be that the breccia represents this portion of the plume and is extruded at this early juncture. The remainder of the less enriched material may pond at shallower levels in the form of a magma chamber. Huppert and Sparks consider that some of this material which is injected is likely to be trapped by the cooler brittle upper crust once it has passed through the more ductile lower crustal rocks. This system may become closed as a result of this and because the magmas from which A-type rocks are generated are at high temperatures 900-1100 °C (Creaser and White, 1991), it is likely that some assimilation of the wall rocks will result in association with a process of differentiation.

There are a number of ways interaction between wall rock and magma may occur, however only two of these relate to this case as they occur in a magma chamber and require heat from the magma itself. The first of these is all parts of a chamber, floor, roof and walls as a result of their melting temperature being exceeded, can be mixed in to contaminate the melt. The second is stoping of the roof with blocks of material becoming assimilated by total melting (Wilson, 1987). This process was modelled using an equation modified from the original proposed by DePaolo (1981). Initially an average Archean crustal composition was used as the contaminant, but results from this were unsatisfactory. Instead a variety of more incompatible trace elements were used, with the metasediments from the study area used as contaminants[1]. The elements used were Zr, Nb, Y and Ce which while not conclusively proving the process which is not possible since the model is highly idealised, did provide some consistent results. The major

[1] For equation used and D values for each of the elements used see Appendix 5

parameters of this process are the r value which is the ratio of assimilation to fractionation. Where r=1 is zone refining or total assimilation occurs which is unlikely to occur and where r=0 pure fractional crystallisation is the result. The other parameter is F, which is the fraction of the magma remaining or the amount of fractional crystallisation which has occurred. In order to produce the composition seen in the rhyodacite, for Zr, Nb and Y 40% fractional crystallisation was necessary, with r values of .6, .3 and .3 respectively. The results for Nb were 50% fractionation and a r value of .5. So on the whole the r values vary slightly while the F values are very consistent.

The fact that fractional crystallisation has played a major role in the development is seen in figure 8.3 showing various trace elements trace elements versus Zr. These show consistent patterns in terms of their ratios and Wilson op cit. equates this with trends of fractionation. If assimilation has played a role the contamination could account for the variation of $^{143}Nd/^{144}Nd$ ratios between the rhyodacite and amphibolites which would be expected to be the same if they were derived from the same source. The fact that evolution of the felsic rocks occurred in a closed system may also account for the absence of intermediate rocks in the area. The bimodality may also be accounted for by a renewed pulse of mantle material into the magma chamber leading to the extrusion of the rhyodacite, the basaltic material would be extruded subsequent to this before it could be differentiated to any large degree. The εNd value of .88 at 1740 indicates a short protolith pre-history of < 100 Ma as identified by McCulloch (1987) for rocks from Archean terrains, suggesting that partial melting of pre-existing Archean crust is a less likely scenario than AFC.

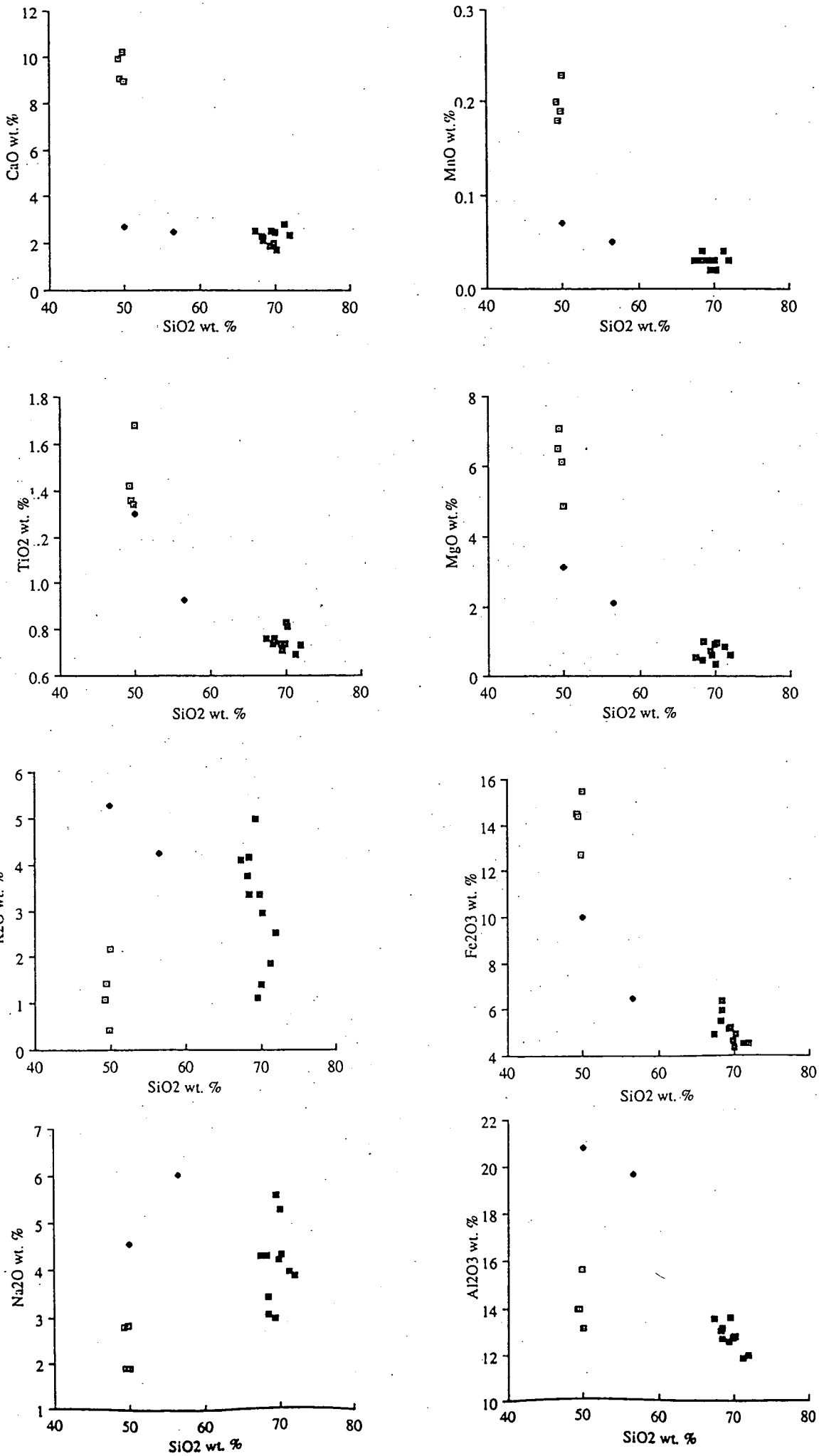

Figure 8.1 Major element versus SiO_2 variation diagrams
(Closed squares rhyodacites, open squares

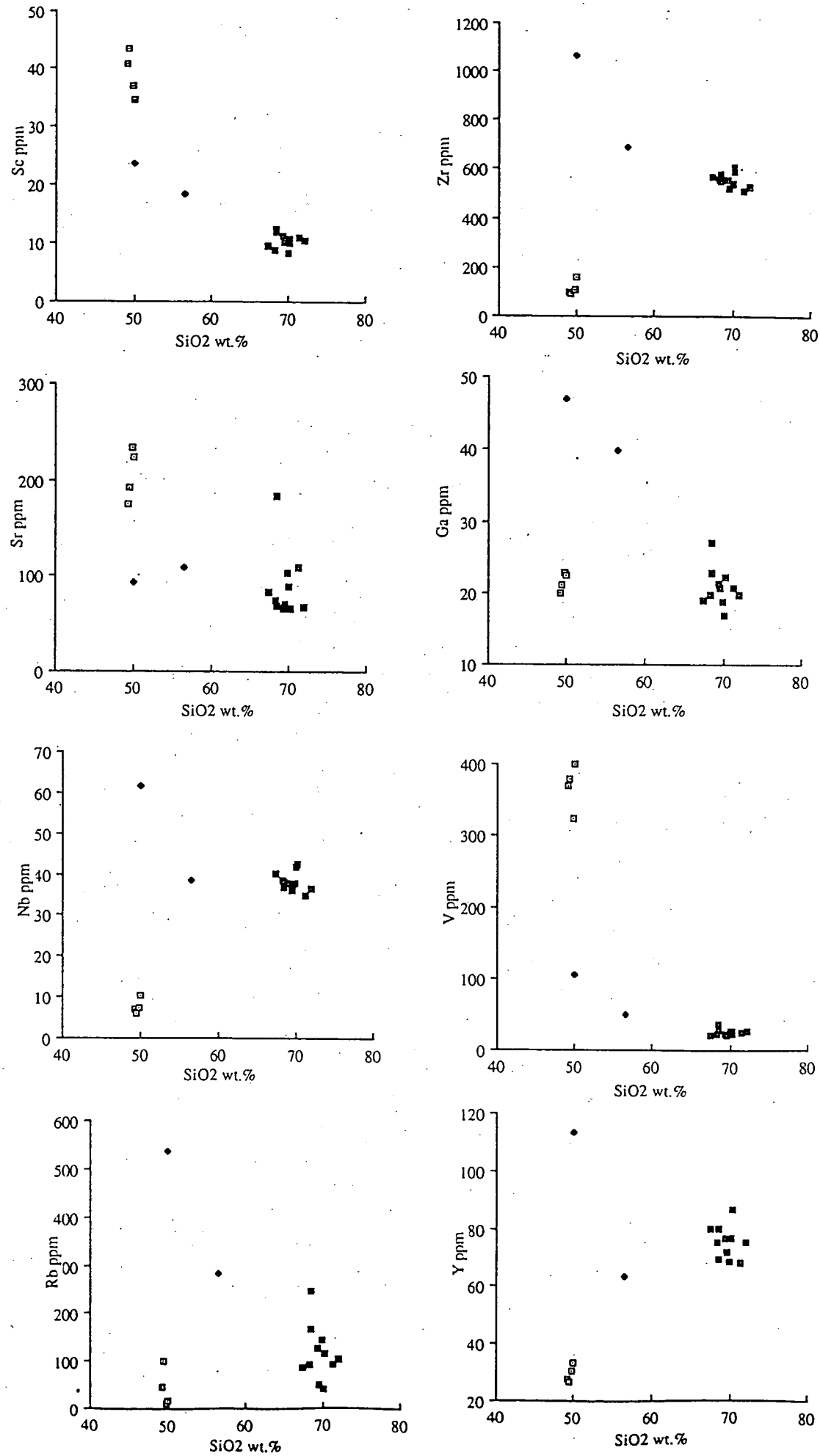

Figure 8.2 Trace element versus SiO_2 variation diagrams
(Closed squares rhyodacites, open squares
amphibolite and diamonds represent breccias).

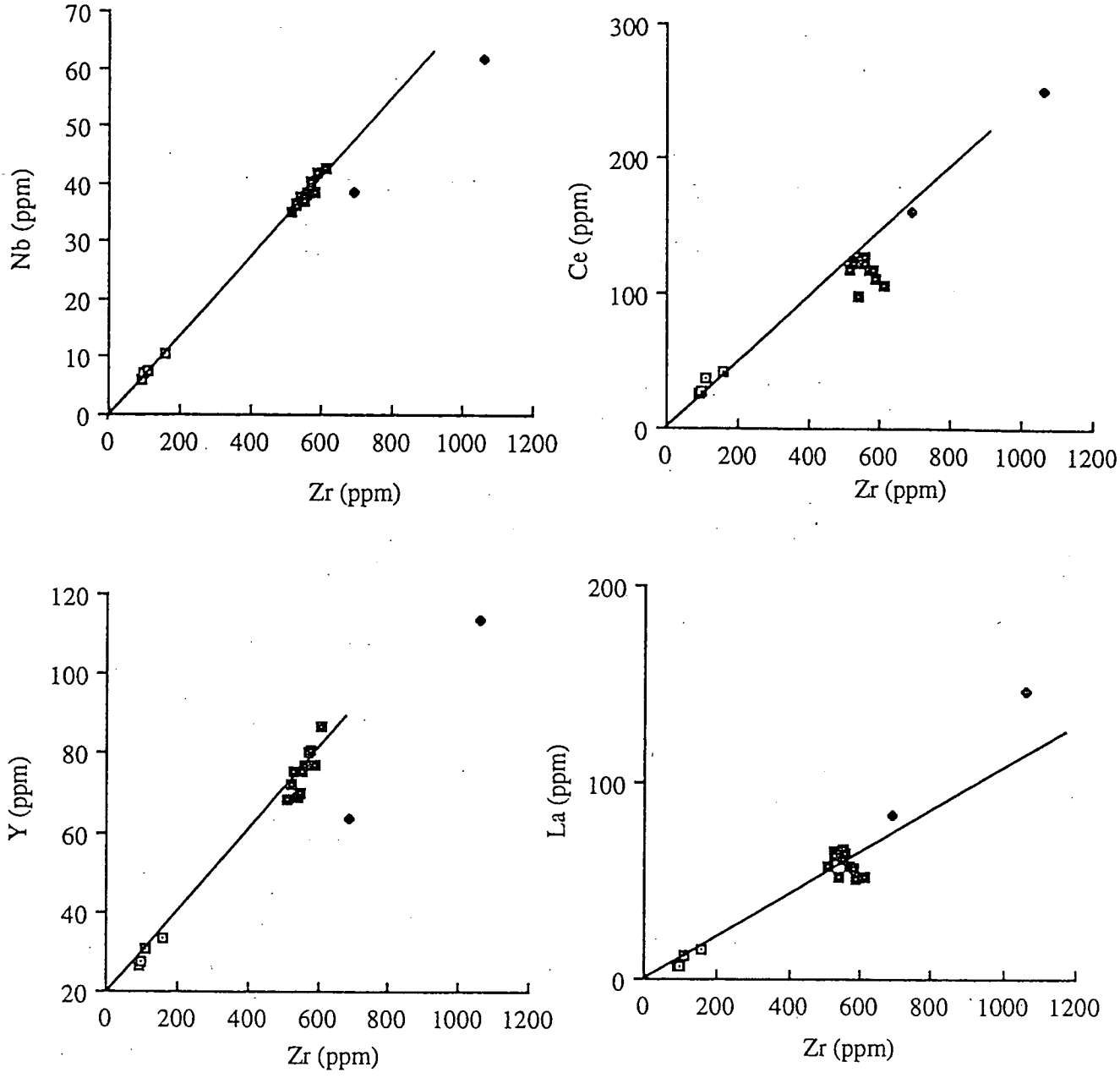

Figure 8.3 Incompatible element plots showing fractionation trends. Open squares amphibolites, closed squares rhyodacites and closed diamonds Breccia clasts.

Conclusions

It is proposed that the suite of felsic metavolcanics and sediments at Pt. Victoria were erupted and deposited in a subaqueous environment, probably a marginal basin. This is supported by the presence of jigsaw fit hyaloclastite breccias which according to Cas (1992) are good indicators of such an environment. The depth of eruption must have been such that the hydrostatic pressure prevented explosive activity.

The tectonic environment is considered on the basis of the tholeiitic nature of the basic rocks and the incompatible enriched A-type character of the felsic rocks to be a intra plate environment. Both of these rock types are commonly found in association with the above mentioned environment. Further support for the tectonic environment is provided by the plots of the rhyodacites on incompatible trace element discrimination diagrams where they lie in the within plate field. This would seem to discount Parkers (1990) suggestion that the Moonta subdomain developed as a subducting arc accreting to the margin of the Gawler Craton. The fact that the suite is not calc-alkaline, a common character of modern arc settings also negates such a possibility.

In terms of the comparative geochemistry of both the felsic and basic rocks in a regional context, comparisons with other Palaeo, Meso and Neo Proterozoic volcanic units indicate that while the mantle source in the Proterozoic had a similar character leading to the abundance of anorogenic suites it was not homogenous. It is more likely based on the variations in element values in both a spatial and temporal sense that nature of the mantle in the Proterozoic was enriched but heterogeneous in character.

With regard to the petrogenesis and source of the rhyodacites, trace element modelling and other data such as consistent incompatible element ratios between the felsic and basic rocks led to the conclusion that they are derived by the fractional crystallisation of a mantle derived magma. This occurred in a high level magma chamber with accessory assimilation of crustal material. Other models of A-type generation were considered but the evidence in favour of these was not as strong as it was for Assimilation and Fractional Crystallisation. The temperature of the felsic product of this process is considered to have been at a very high temperature in excess of 900° C because of the high levels of incompatible elements particularly Ga and Zr. This is because they form complexes within a melt which are only stable at high temperatures. In terms of crustal generation in the Proterozoic, it has been shown that the rocks at Pt. Victoria are produced from a mantle derived magma supporting the notion that this was a period of generation of new crustal material with minimal incorporation of the existing Archean crust.

Acknowledgements:

I would like to begin by thanking my supervisor John Foden who gave me the chance to undertake this project, his advice and willingness to answer any questions has been appreciated. All the technical staff, David Bruce for his patience and assistance with isotope analysis, John stanley for XRF analysis, Sherry Proferes for drafting, Wayne Mussared and Geoff in the Lapidiary and Keith Turnbull. Jo Mawby and Annette Bingemer for reading and advice on initial drafts. Leigh Rankin from SADME for providing geochemical data for comparison. Many thanks goes to my fellow Honours students and friend who have made this year not only bearable, but enjoyable. Most thanks goes to my family, especially my parents who gave me the opportunity to further my education at tertiary level and have always been there when I needed them.

References

Bone, Y., (1978). The geology of Wardang Island, Yorke Peninsula. S.A. **B.Sc. (Hons.) thesis University of Adelaide** (unpublished).

Bone, Y., (1984). The Wardang Volcanics, Wardang Island, Yorke Peninsulsa, S.A. **Quarterly Geological notes, Geological survey of South Australia,** 89, pp. 2-7.

Cas, R.A.F. & Wright, J.V., (1987). **Volcanic Successions, Modern and ancient, A gelogical approach to processes, products and successions.** Allen & Unwin, London.

Cas, R.A.F., (1992). Submarine Volcanism: Eruption Styles, Products and Relevance to Understanding the Host Rock Successions to Volcanic Hosted Massive Sulfide Deposits. **Economic Geology**, 87, pp 511-541.

Chappell, B.W. and White, A.J.R., (1992). I- and S-type granites in the Lachlan Fold Belt. **Transactions of the Royal Society of Edinburgh: Earth Sciences**, 83, 1-26.

Chappell, B.W., (1984). Source rocks of I- and S-type granites in the Lachlan Fold Belt,S.E. Australia. **Phil.trans. R.Soc.Lond.**, A310, 693-707.

Collins, W.J., Beams, S.D., White, A.J.R., and Chappell, B.W., (1982). Nature and Origin of A-Type Granites with Particular Reference to Southeastern Australia. **Contrib. Mineral. Petrol.**, 80, 189-200.

Cox, K.G., Bell, J.D., & Pankhurst, R.J., (1979). **The Interpretation of Igneous Rocks**. George Allen & Unwin, London.

Creaser, R.A. and White, A.J.R., (1991). Yardea dacite large volume, high temperature volcanism from the middle Proterozoic of South Australia. **Geology**, 19, 163-166.

Creaser, R.A., (1989). **The geology and petrology of Middle Proterozoic felsic magmatism of the Stuart Shelf, South Australia**. Ph.D.thesis, La Trobe University, (unpublished).

Creaser, R.A., Price, R.C., & Wormald, R.J., (1991). A-type granites revisited: Assessment of a residual source model. **Geology**, vol. 19, pp. 163-66.

Etheridge, M. , Rutland, R., and Wyborn, L., (1987). Orogenesis and tectonic process in the early to middle Proterozoic of Northern Australia, **Proterozoic Lithospheric Evolution, Geodynamics series**, v 17, 131-147.

Fanning, C.M., (1985). Comments on Rb-Sr total rock dating measurements for the Wardang Volcanics, Yorke Peninsula. **Quarterly Geological notes, Geological survey of South Australia,**

Fanning, C.M., Flint, R.B., Parker, A.J., Ludwig, K.R. amd Blisset, A.H., (1988). Refined Proterozoic evolution of the Gawler Craton, South Australia, Through U-Pb Zircon Geochronology. **Precambrian Research**, vol. 40/41, pp. 363-386.

Foden,J.D., (1992) Personal Communication Department of Geology and Geophysics Adelaide University

Giles, C.W. & Teale, G.S., (1979). A comparison of the geochmistry of the Roopena volcanics and the Beda volcanics. **Quarterly Geological notes, Geological survey of South Australia**, no.71, pp 7-12.

Giles, C.W., (1980). **A study of PreCambrian Felsic Volcanism in Southern Australia**, Ph.D.thesis. University of Adelaide, (unpublished).

Hafer, M.R., (1991). **Origin and Controls of Deposition of the Wheal Hughes and Poona Copper Deposits, Moonta, South Australia.** Honours thesis, University of Adelaide, (unpublished).

Loiselle, M.C. and Wones, D.R., (1979). Characteristics and origin of anorogenic granites. **Geological Society of America Abstracts with Programs**, 11, pg. 468.

McCulloch, M.T., (1987). Sm-Nd constraints on the evolution of Precambrian crust in the Australian continent. **Proterozoic Lithospheric Evolution, Geodynamics series**, v.17, 115-130.

McIntyre, G.A., Brooks,C., Compston, W. and Turek, A., (1966). The statistical assesment of Rb-Sr Isochrons. **Journal of Geophysical Research**,71: 5459-5468.

Parker, A.J. & Lemon, N.M., (1982). Reconstructionof the Early Proterozoic Stratigraphy of the Gawler Craton, South Australia. **Journal of the Geological Society of Australia**, 29, pp 221-38.

Parker, A.J., (1990). Gawler Craton and Stuart Shelf- regional geology and mineralisation. In Hughes, F.E. (Ed.), **Geology of the mineral deposits of Australia and P.N.G, Vol. 1**, Australasian Institute of Mining and Metallurgy.

Pearce, J.A. & Norry, M.J., (1979). Petrogenetic implications of Ti, Zr, Y, and Nb variations in volcanic rocks. **Contributions to Mineralogy and Petrology**, 69, pp 33-47.

Pearce, J.A. amd Cann, J.R., (1973). The tectonic setting of basic volcanic rocks determined using trace element analyses. **Earth and Planetary Science Letters**, 19, pp 290-300.

Pearce, J.A., Harris, N.B.W. and Tindle, A.G., (1984). Trace element discrimination digrams for the tectonic interpretation of granitic rocks. **Journal of Petrology**, vol. 25, part 4, pp. 956-983.

Plimer, I.R. (1980). **Moonta-Wallaroo District, Gawler Block, South Australia: Areview of the geology, ore deposits and untested potential of EL 544.** North Broken Hill Report, S.A.D.M.E. (unpublished report).

Stewart, K Ph.D. High temperature felsic volcanism and the role of mantle magmas in proterozoic crustal growth: the Gawler Range Volcanics Ph.D. thesis University of Adelaide (unpublished)

Sun, S.S and McDonough, W.F., (1989). Chemical and Isotopic systematics of oceanic basalts: implications for mantle compositions and processes. In Saunders, A.D. and Norry, M.J. (eds) 1989, **Magmatism in ocean basins**. Geological Society Special Publications. 42, pp 313-345.

Turner, S., Foden, J., Sandiford, M. and Bruce, D. (1993). Sm-Nd evidence for the provenance of sediments from the Adelaide Fold Belt and southeastern Australia with implication for episodic crustal addition. **Geochimica et Cosmochimica Acta**, Vol. 57, pp. 1837-1856.

Webb, A.W., Thomson, B.P., Blisset, A.H., Daly, S.J., Flint, R.B. & Parker, A.J., (1986). Geochronology of the Gawler Craton, South Australia. **Australian Journal of Earth Sciences**, 33, pp 119-143.

Whalen, J.B., Currie, K.L and Chappell, B.W., (1987). A-type granites: geochemical characteristics discrimination and petrogenesis. **Contributions to Mineralogy and Petrology**, 95, pp 407-419.

Wilson, M., (1987). **Igneous Petrogenesis**, Unwin Hymam, London.

Wyborn, L.A.I, Wyborn, D, Warren, R.G. and Drummond, B.J., (1992). Proterozoic granite type in Australia: implications for lower crust composition, structure and evolution. **Transactions of the Royal Society of Edinburgh: Earth Sciences**, 83, 201-209.

Wyborn, L.A.I., (1988). Petrology, Geochemistry And Origin Of A Major Australian 1880-1840 Ma Felsic Volcano-Plutonic Suite: A Model For Intracontinental Felsic Magma Generation. **Precambrian Research**, v. 40/41, 37-60.

Wyborn, L.A.I., Page, R.W. and McCulloch, M.T., (1988b). Petrology, geochronology and isotope geochemistry of the post-1820 Ma granites of the Mount Isa Inlier: mechanisms for the generation of Proterozoic anorogenic granites. **Precambrian Research**, v. 40/41, 509-541.

Wyborn, L.A.I., Page, R.W. and Parker, A.J., (1987). Geochemical and geochronological signatures in Australian Proterozoic igneous rocks. In Pharaoh,T.C., Beckinsale, R.D. and Rickard, D. (Eds.) 1987, **Geochemistry and Mineralization of Proterozoic Volcanic Suites**, Geological Society Special Publication No. 33, pp. 377-394.

Appendices

Appendix 1 : Thin Section Descriptions.

Rhyodacite: Sample No. 1002-19

Porphyritic, extremely fine grained matrix of predominantly quartz and some feldspar seen as microcline and plagioclase. Biotite and hornblende also make up important components of the matrix, and are both related. The phenocryst assemblage is heavily altered, with many of them only being able to be recognised by outlines due to the extensive alteration by mainly sericite, some however can be recognised by remnant twinning. Sphene also makes up a proportion of the mode seen as euhedral but mainly anhedral crystals. Opaques represented by magnetite are disseminated throughout the whole section. the fact that the matrix is so fine and metamorphic crystallisation so evident by 120 degree triple points, it must have almost been a glass prior to this. Hornblende and biotite are seen to align most likely as a result of metamorphism. The feldspars in the matrix are not as altered as those making up the phenocryst assemblage

Mineral	%age
Quartz	30 %
Feldspar (phenocryst and matrix)	25 %
Hornblende	20 %
Biotite	10 %
Sphene	5 %
Sericite	5 %
Opaques (Magnetite)	5 %

Rhyodacite: Sample No. 1002-94

Porphyritic, feldspars are highly altered with sericite being a common alteration mineral. Despite being altered can still ascertain what their character is by remnant twinning which is obvious. Microcline, K-spar and plagioclase recognised by cross hatching, Carlsbad and multiple twinning respectively. All the feldspars are anhedral-subhedral with the margins corroded by the matrix development. Biotite is present as small anhedral crystals, however there are some longer bladed crystals present. Hornblende is more abundant and is seen as anhedral crystals and is present as embayments in both the phenocrysts and the matrix. Opaques seen as magnetite are also present as subhedral crystals. Accessory phases which are seen are both fluorite and apatite

Mineral	%age
Quartz	35%
Feldspar	30%
Biotite	15%
Hornblende	5
Opaques (Magnetite)	5 %
Fluorite	<1 %
Rutile	<1 %

Rhyodacite: Sample No. 1002-84

Porphyritic, less altered than most of the samples looked at, the phenocryst assemblage is easily recognised as being composed of plagioclase, K-spar and some microcline with the alteration effects not being as recognisable. These range in size from 1-4 mm and are anhedral. The matrix is fine grained and composed and composed of predominantly feldspars, subhedral crystals of K-spar and microcline as well as plagioclase of <3 mm. Quartz is also seen in the matrix but and is present as round anhedral crystals associated with the feldspars. Biotite is also a matrix component but minor to the above mentioned constituents, it occurs as small blades and larger anhedral crystals up to .5 mm. The biotite is also seen to wrap around phenocrysts defining a foliation. Hornblende is also a minor matrix component, opaques seen as magnetite are dispersed throughout the matrix with some euhedral crystals but the majority are subhedral. Fluorite and apatite are both seen as accessory phases in minor amounts, many of the apatites are euhedral.

Mineral	%age
Feldspars (phenocryst)	26 %
Feldspars (matrix)	30 %
Biotite	15 %
Quartz	10 %
Opaques (Magnetite)	7 %
Sericite	6 %
Hornblende	3 %
Apatite	<1 %
Fluorite	<1 %

Rhyodacite: Sample No. 1002-14

Porphyritic, phenocryst assemblage of feldspars heavily sericitised and altered, but remnant twinning (cross hatching) identifies them as microcline, these are subhedral due to the embayment of the matrix around the edges of the crystals and are up to 4 mm in size. In places the phenocrysts have been completely psuedomorphed by quartz and feldspars from the matrix. The matrix is composed mainly of subhedral feldspars and quartz. The feldspars in the matrix are dominantly microcline with some plagioclase. Biotite and hornblende are also preset in the matrix with biotite being more common, with blade crystals of ~.2 mm, these define a foliation. Opaques represented by magnetite are dispersed throughout the matrix. Accessory minerals in minor proportions are apatite and fluorite.

Mineral	%age		
Feldspar (phenocryst)	10 %	Sericite	5 %
Feldspar (matrix)	40 %	Apatite	<1 %
Quartz	25 %	Fluorite	<1 %
Biotite	15 %		
Hornblende	5 %		

Amphibolite: Sample No. 1002-16

Section is dominated by hornblende, seen as pale green to green subhedral to anhedral crystals of varying sizes and identified by the 120 degree cleavage. Secondary to the hornblende is plagioclase showing multiple twinning and represented by anhedral to subhedral crystals ranging in size from .5-3 mm, with many partially corroded by sericite. Sphene is another doninant phase after plagioclase and hornblende and is generally subhedral with crystals up to 2 mm. Biotite is seen as anhedral bladed crystals which are spread through the section and occur singularly. Quartz is a minor component and occurs as both agglomerations of crystals and on their own. Rutile is also present as a minor accesory phase.

Mineral	%age
Hornblende	50 %
Plagioclase	30 %
Sphene	10 %
Quartz	5 %
Biotite	4 %
Rutile	<1 %
Sericite	<1 %

Amphibolite: sample No. 1002-9

Hornblende is the dominant mineral present, seen as light brown to dark green in plain light with the characteristic 120 degree cleavage. It occurs as anhedral crystals ranging in size up to 2 mm. Feldspars are also present but have been extensively altered evidenced by the presence of sericite, however remnant multiple twins can be seen identifying them as plagioclase. Biotite is seen as anhedral lathes which are <1 mm. Chlorite which is also present forms radiating aggregates and seems to be forming after the biotite. Sphene is seen as anhedral crystal and are often associated with the opauques which could be titanomagnetite. Quatrz is present as anhedral crystal, with rutile and apatite being present as accessory phases.

Mineral	%age
Hornblende	25 %
Plagioclase	7 %
Chlorite	15 %
Quartz	10 %
Sericite	8 %
Sphene	5 %
Biotite	5 %
Opaques	<1 %
Rutile	<1 %

Amphibolite: Sample No. 1002-5

Dominant mineral is hornblende seen as brown to dark brown anhedral and subhedral crystals up to 2 mm. Feldspars have also been a dominant phase but these have been totally sericitised and their original character is unknown though it is thought to have been plagioclase. Opaques are common and are mostly seen rimmed by anhedral crystals of sphene. Quartz is also seen as subhedral crystals and in this particular section forms a vein with crystals up to 4 mm, and recognised as metamorphic by composite stressed grains. Biotite also forms a minor component with bladed anhedral crystals of around .5 mm.

Mineral	%age
Hornblende	60 %
Quartz	15 %
Sericite	10 %
Opaques	8 %
Sphene	7 %
Biotite	<1 %

Breccia Clast: Sample No.1002-78

Porphyritic with phenocryst assemblage dominated by feldspars, microcline, K-spar and minor plagioclase. All are anhedral which is possibly a result of cotrrosion or resorbtion, as alteration of all the phenocrysts by sericite is obvious. Many of the feldspar phenocrysts form agglomerates indicative of a glomeroporphyritic texture. The matrix is extremely fine grained and composed of equigranular quartz and minor feldspar. Biotite however is the dominant component with minor amounts of allanite which has been retrograded to chlorite. Epidote rims on some of the allanite crystals would support hyrothermal alteration. Opaques represented by magnetite make up a fair proportion of the section, indicating low temperature phases. Other observed minor accessory minerals are euhedral apatites and some minor fluorite, hornblende is also a minor phase,as is calcite.

Mineral	%age
Biotite	40 %
Feldspars	25 %
Quartz	20 %
Sericite	5 %
Opaques (Opaques)	5 %
Allanite	<2 %
Chlorite	<1 %
Epidote	<1 %
Fluorite	<1 %
Hornblende	<1 %
Calcite	<1 %

Breccia Clasts: Sample No. 1002-72

Altered porphyry assemblage made up of altered and corroded feldspars dominated by microcline, these range in size from 2-4 mm. Feldspars also make up a large proportion of the matrix, which cinsists of subhedral crystals of microcline with some plagioclase. Biotite is also prominent in the matrix and occurs as both single anhedral crystals and as aggregates of numerous crystals. Hornblende is also present in association with the biotite. Quartz as mentioned is found in the matrix as fine grained crystals of .1-.3 mm. Sphene is also present as subhedral grains both on its own and after pyrite and magnetite, the size of these varies from quite small crystals up to .2 mm. Opaques as mentioned are seen by pyrite and magnetite as anhedral crystals and are not limited to the matrix but are seen as overgrowths on the feldspars. Apatite is also seen as a minor phase, dispersed throughout the matrix.

Mineral	%age
Feldspar	36 %
Biotite	30 %
Quartz	10 %
Sphene	10 %
Hornblende	4 %
Apatite	3 %
Opaques (Magnetite)	5 %
Pyrite	2 %

Breccia Matrix: Sample No. 1002-57

Fine grained agglomeration of quartz, feldspar and biotite, alteration has occurred by sericitisation of the feldspars. Quartz is dominant and shows undulose extinction, occurring as rounded and anhedral crystals. The feldspars are represented by anhedral of microcline which in general are quite small, but range up to .7 mm in size. Biotite is also present as bladed crystals which do not seem to show any preferred orientation. some biotites show alteration by epidote. Accessory minerals are epidote as mentioned as well as fluorite and apatite, both are seen as euhedral crystals. Thre is also some minor chlorite after biotite. Magnetite is also seen as anhedral crystals dispersed throughout the section.

Mineral	%age
Quartz	40 %
Feldspar	30 %
Biotite	30 %
Opaques (Magnetite)	2 %
Epidote	<1 %
Fluorite	<1 %
Apatite	<1 %
Chlorite	<1 %

Metasediment: Sample No. 1002-6

The dominant mineralogy is quartz which is represented by a wide range of crystal sizes which are anhedral, many of the larger crystals are embayed. There are also a number of represented by microcline. Biotite is also prominent, seen generally as anhedral lathes, muscovite also is a common mineral seen as large anhedral embayed crystals which formed as a late stage mineral, these range in size from 2-4 mm. Quartz is the most common embayed mineral and there are reaction rims in the muscovite as it has grown around these. Accessory minerals are zircons, recognised as inclusions in biotite crystals by radiation haloes around them. Rutile is also present in trace amounts, as are opaques.

Mineral	%age
Quartz	40 %
Biotite	25 %
Muscovite	20 %
Feldspar	11 %
Opaques	3 %
Zircon	<1 %
Rutile	<1 %

Metasediment: Sample No. 1002-34

Component minerals are bladed subhedral crystals of biotite which show a rough alignment delineating a fabric, which is likely a product of metamorphism. Hornblende is also present and shows a similar relationship to the biotite and is predominantly represented by subhedral crystals bounded by feldspar and quartz. The feldspars are the dominant constituent in the section, most of which show the cross hatched tartan twinning of of microcline, most of these are anhedral crystals and show alteration by sericite. Quartz is minor to the feldspars and is seen to bound them as enbayments. Large muscovite crystals are present and show poikiloblastic textures, these probably form as a result of a late satge retrograde reaction. Apatite also occurs as an accessory phase and is represented by round euhedral crystals.

Mineral	%age
Feldspar	45 %
Hornblende	20 %
Biotite	15 %
Quartz	15 %
Muscovite	5 %
Apatite	<1 %

Metasediment: Calc-silicate Layer, Sample No. 1002-13

This is a calcsilicate layer which contains scapolite, with clinopyroxene being the dominant mineral with hornblende after it, this is represented by subhedral grains up to 4 mm in diameter, and is being replaced by hornblende. The scapolite is represented by large anhedral crystals associated with rounded quartz crystals showing straight extinction. The quartz is also seen as large anhedral crystals of up to 1.5 mm. The scapolite seems to have grown around the quartz and shows poikiloblastic textures. Sphene also occurs as euhedral and anhedral crystals. Calcite is also present as subhedral crystals ranging in size from .5-1 mm and identified by its birdseye extinction. Opaques are also a minor accessory phase seen as anhedral crystals. Rounded apatite crystals are also seen in trace amount.

Mineral	%age
Scapolite	30 %
Quartz	29 %
Clinopyroxene	22 %
Calcite	5 %
Sphene	4 %
Hornblende	3 %
Opaques	2 %
Apatite	<1 %

Metasediment: Interlayer, Sample No. 1002-13

This layer is predominantly composed of feldspar and quartz. The feldspar is represented by anhedral crystals of microcline seen by the cross hatched twins of up to .5 mm. The quartz is much less abundant than the feldspar and is seen as rounded anhedral crystals. Hornblende is also abundant being present as subhedral crystals up to 1 mm, and being dark to light green in plain light. Calcite seems to be a secondary mineral growing as single anhedral crystals and in veins. Sphene is an accessory phase seen as small .1 mm anhedral and diamond euhedral shaped crystals.

Mineral	%age
Feldspar	45 %
Hornblende	30 %
Quartz	17 %
Sphene	5 %
Calcite	3 %

Appendix 2

XRF Whole Rock Analysis Results

Amphibolites

Sample Numbe	1002-56	1002-47	1002-35	1002-93
SiO2	49.31	49.8	49.99	49.12
Al2O3	13.96	15.66	13.15	13.96
Fe2O3	14.4	12.7	15.48	14.48
Mn0	0.18	0.19	0.23	0.2
MgO	7.09	6.13	4.87	6.51
CaO	9.04	10.18	8.9	9.88
Na2O	1.92	2.81	1.92	2.79
K2O	1.44	0.42	2.18	1.08
TiO2	1.36	1.34	1.68	1.42
P2O5	0.16	0.17	0.19	0.16
SO3	0.03	0.01	0.07	0.03
LOI	1.17	0.54	0.61	0.62
TOTAL	100.07	99.95	99.29	100.25
Y	26.5	30.7	33.6	27.7
Sr	191.8	233.8	224	174.9
Rb	101.1	11.3	17.6	44.8
Nb	6	7.4	10.4	7.1
Zr	89.5	108.3	157	97.3
Th	1.6	3.7	2.9	2.6
Pb	5.3	4.5	2.1	3.4
U	0.4	0.7	-1.4	1
Ga	21.1	22.9	22.5	20
Cu	134	39	83	163
Zn	97	100	108	86
Ba	113	46	133	143
Sc	43.3	37	34.5	40.7
V	379.5	323.1	399.9	369.3
Cr	244	183	73	246
Ni	105	69	60	85
Ce	26	37	42	27
Nd	8	13	12	4
La	7	12	15	6

Metasediments

Sample Numbe	1002--31	1002-7	1002-36	1002-25	1002-37
SiO2	64.73	63.86	66.86	66.1	66.94
Al2O3	16.31	16.07	14.64	15.09	14.58
Fe2O3	5.59	6.05	4.68	5.7	4.7
MnO	0.05	0.07	0.05	0.05	0.08
MgO	2.23	2.43	2.09	2.23	2.29
CaO	1.19	1.49	1.21	1.39	2.26
Na2O	2.01	2.84	3.13	1.76	2.31
K2O	5.24	5.65	5.76	5.26	4.78
TiO2	0.63	0.6	0.6	0.62	0.55
P2O5	0.05	0.11	0.15	0.05	0.14
SO3	0	0.01	0	0	0
LOI	1.38	0.49	0.4	1.07	0.88
TOTAL	99.4	99.67	99.57	99.34	99.52
Y	20	24.6	24.2	20	24
Sr	191.9	266.9	100.5	161.9	138.5
Rb	268.8	274.7	242.7	271.4	261.7
Nb	15.6	15.4	12.6	14.7	13.4
Zr	181.1	183.5	290.4	214.5	220.5
Th	13.8	15.7	15.6	13.8	17.4
Pb	5.7	10.8	5.5	2.6	3.7
U	1.9	2.4	1	-0.1	1.5
Ga	26.4	24.5	23.9	22.7	23.2
Cu	3	4	5	8	7
Zn	55	88	59	45	67
Ba	916	800	729	855	829
Sc	15.2	17.3	12.5	14.3	12.9
V	64.957	79.1	63.8	66.3	57.3
Cr	87	99	74	79	67
Ni	39	43	38	40	36
Ce	57	71	76	50	90
Nd	26	30	34	21	41
La	27	35	36	27	47

Sample Numbe	1002-13	1002-13a	1002-13b	1002-13c	1002-13d
SiO2	62.87	63.93	66.15	63.26	65.82
Al2O3	11.21	12	12.23	11.76	12.58
Fe2O3	5.41	4.75	3.89	4.67	3.88
MnO	0.17	0.16	0.08	0.14	0.07
MgO	2.43	2.15	2.15	2.2	2.23
CaO	12.61	10.24	4.34	11.87	4.32
Na2O	2.54	2.43	1.01	2.72	1.23
K2O	0.32	1.94	8.27	0.61	7.85
TiO2	0.41	0.52	0.59	0.52	0.56
P2O5	0.17	0.17	0.16	0.18	0.16
SO3	0.19	0.15	0.01	0.15	0.02
LOI	0.66	0.54	0.65	0.73	0.85
TOTAL	99.01	98.96	99.54	98.82	99.57
Y	33.1	27.4	18.2	33.3	20.9
Sr	80.4	101.3	132.4	91.8	128.5
Rb	13.1	117.1	533.1	31.1	471.6
Nb	12.6	11.9	14.4	12.6	13.4
Zr	386.9	279.1	306.2	264.4	305.6
Th	17.3	13.5	15.5	16.7	15.8
Pb	7	4.4	6.4	5.2	5.7
U	6.5	6.9	7	10.6	7.8
Ga	16.5	16.9	19.8	18.9	17.9
Cu	8	1	8	8	11
Zn	38	35	36	40	36
Ba	31	437	1118	113	854
Sc	6.8	7.6	7.6	8	8.5
V	52.2	84.3	107.3	89.6	105.4
Cr	36	61	66	52	62
Ni	28	30	33	27	33
Ce	97	75	71	93	87
Nd	41	33	32	41	40
La	50	36	34	48	45

Pegmatites

Sample Number	1002-26	1002-60	1002-83
SiO2	67.79	74.91	76.01
Al2O3	17.24	13.71	13.84
Fe2O3	0.62	0.51	0.34
MnO	0.01	0	0
MgO	0.56	0.08	0.07
CaO	0.45	0.4	0.64
Na2O	2.98	3.52	4.32
K2O	8.9	6.08	4.49
TiO2	0.15	0.05	0.05
P2O5	0.02	0	0
SO3	0	0	0
LOI	0.57	0.35	0.26
TOTAL	99.29	99.63	100.02
Y	22.5	42.9	22.4
Sr	212	30.2	30.7
Rb	461.6	516	351.8
Nb	6	59.9	57.3
Zr	60.3	87.3	27.9
Th	28.3	21.7	16.2
Pb	8	4.4	5.4
U	7.1	5.8	11.1
Ga	18.8	30.2	24.4
Cu	10	3	10
Zn	16	10	9
Ba	1065	436	163
Sc	5.9	3.3	3.5
V	21.8	4.4	5.3
Cr	30	18	29
Ni	15	11	12
Ce	10	7	14
Nd	5	8	11
La	4	0	8

	Breccia Matrix		Breccia Clasts	
Sample Numbe	1002-17	1002-89	1002-85	1002-78
SiO2	86.35	76.89	49.99	56.52
Al2O3	6.92	10.52	20.84	19.73
Fe2O3	0.84	3.1	10	6.46
MnO	0.01	0.03	0.07	0.05
MgO	0.2	1.07	3.14	2.11
CaO	0.28	2.16	2.69	2.48
Na2O	1.15	2.52	4.56	6.04
K2O	3.24	2.11	5.27	4.25
TiO2	0.26	0.48	1.3	0.93
P2O5	0.07	0.13	0.46	0.25
SO3	0	0.02	0.01	0.01
LOI	0.45	0.68	0.8	0.68
TOTAL	99.78	99.7	99.15	99.5
Y	12.2	38.7	113.3	63.4
Sr	107.6	53.9	93.6	108.7
Rb	100	143.5	536.7	284.6
Nb	9.3	11.4	61.7	38.4
Zr	158	190	1062.3	690.7
Th	6	11.1	42	29.3
Pb	5.8	10.9	7.6	10.1
U	0.9	19.2	11	8.6
Ga	12.7	17.8	47	39.8
Cu	24	8	0	5
Zn	11	18	49	34
Ba	336	783	968	1020
Sc	4	9.1	23.5	18.3
V	22.1	37.2	105.8	50.4
Cr	56	54	14	9
Ni	15	16	42	20
Ce	32	67	253	162
Nd	17	31	126	74
La	16	34	147	84

Rhyodacites

Sample Numbe	1002-18	1002-33	1003-43	1002-55	1002-61
SiO2	69.98	68.42	72.11	71.4	69.58
Al2O3	12.66	13.05	11.92	11.81	13.53
Fe2O3	4.64	5.99	4.52	4.53	5.2
MnO	0.03	0.04	0.03	0.04	0.02
MgO	0.92	0.99	0.61	0.83	0.62
CaO	1.99	2.15	2.35	2.81	2.5
Na2O	4.21	3.05	3.88	3.96	5.6
K2O	3.36	4.16	2.53	1.88	1.11
TiO2	0.74	0.76	0.73	0.69	0.71
P2O5	0.17	0.18	0.17	0.16	0.18
SO3	0.02	0.01	0.02	0.03	0.01
LOI	0.83	1.02	0.94	1.4	0.87
TOTAL	99.55	99.82	99.82	99.54	99.95
Y	68.9	70	75.5	68.4	72
Sr	102.7	184.2	68	108.7	70.8
Rb	143	246.7	102.8	92.8	47.8
Nb	37.7	36.8	36.6	35	36.2
Zr	542.1	550.3	528.6	512.2	525.9
Th	25.7	25.3	25.1	25.4	24.9
Pb	6.7	4.8	5.4	5.5	5.9
U	5.3	7	7.3	6.2	6.7
Ga	18.8	22.9	19.7	20.8	20.7
Cu	7	9	11	3	7
Zn	24	27	17	26	17
Ba	862	798	686	524	261
Sc	8.4	12	10.5	10.9	10.2
V	26.8	35.5	26.8	24.4	21.8
Cr	23	13	13	20	22
Ni	22	30	16	16	14
Ce	99	128	123	118	124
Nd	41	59	59	55	59
La	52	66	63	58	65

Sample Numbe	1002-66	1002-70	1002-74	1002-75	1002-80
SiO2	68.47	69.31	70.17	70.25	67.46
Al2O3	12.62	12.52	12.75	12.73	13.48
Fe2O3	6.35	5.16	4.37	4.91	4.95
Mn0	0.03	0.03	0.03	0.02	0.03
MgO	0.99	0.74	0.36	0.96	0.54
CaO	2.22	1.92	2.47	1.73	2.53
Na2O	3.43	2.97	5.3	4.32	4.3
K2O	3.36	4.99	1.4	2.97	4.1
TiO2	0.75	0.74	0.83	0.81	0.76
P2O5	0.19	0.18	0.2	0.2	0.19
SO3	0.04	0.03	0.01	0.01	0.02
LOI	0.97	0.81	1.52	0.66	1.28
TOTAL	99.41	99.39	99.41	99.57	99.63
Y	80.5	76.8	76.8	86.8	80.1
Sr	68.5	66	89.7	65.8	83.9
Rb	165.4	126.8	39.5	114.2	86.3
Nb	38.2	37.9	41.7	42.4	40.2
Zr	580.8	559.3	590.9	611.1	570.5
Th	22.8	25	26.7	25.6	27.3
Pb	5.6	4.9	3.6	6.6	6.4
U	7	7.9	7.4	8.8	7.5
Ga	27	21.2	16.8	22.2	18.9
Cu	20	16	11	8	9
Zn	18	32	14	16	17
Ba	1126	1049	433	662	1130
Sc	12.5	11.3	10	10.7	9.5
V	28.6	22.9	26.4	22.2	21.2
Cr	3	15	25	35	34
Ni	11	14	17	28	26
Ce	117	128	112	106	117
Nd	57	61	55	47	54
La	56	64	51	52	58

Moonta Porphyry Samples

Sample Numbe	1002-97	1002-BDDH	1002-MP680	1002-YL246	1002-YL340
SiO2	68.3	71.76	71.74	73.69	70.13
Al2O3	12.97	11.96	12.29	12.84	11.89
Fe2O3	5.49	4.84	4.97	2.87	6.29
MnO	0.03	0.04	0.04	0.01	0.04
MgO	0.47	0.59	2.08	0.28	1.97
CaO	2.29	0.2	0.21	0.29	0.26
Na2O	4.31	2.29	3.43	4.98	3.56
K2O	3.76	5.82	2.93	3.5	4.28
TiO2	0.74	0.56	0.55	0.52	0.5
P2O5	0.18	0.07	0.07	0.09	0.07
SO3	0.02	0	0	0	0
LOI	1.21	1.31	1.51	0.44	0.55
TOTAL	99.78	99.43	99.8	99.5	99.53
Y	75.4	84.1	95.9	138.7	91.5
Sr	74.7	34.1	21.2	27.2	33.8
Rb	92.1	165.7	99.8	84.2	215.7
Nb	38.4	46.6	45.8	45.9	44.2
Zr	554.6	583.1	586.7	581.5	560.6
Th	25.5	41.1	43.8	61.7	39.6
Pb	17.6	3.6	4.7	5.7	3.2
U	5.5	17.9	9.6	14.7	11.3
Ga	19.7	24.2	27.9	19.8	27.3
Cu	7	12	8	66	25
Zn	24	20	33	12	22
Ba	864	1337	537	756	932
Sc	8.7	11.5	16.6	7.7	14.3
V	22.9	7.6	9.7	5.6	9.2
Cr	16	15	22	5	63
Ni	15	10	31	27	38
Ce	122	192	31	307	46
Nd	58	91	13	143	28
La	61	97	9	161	18

Appendix 3 :

1. Sample Preparation for XRF Whole Rock Analysis:

Samples were prepared as follows:

a) To obtain fresh sample material all the weathered surfaces were removed.

b) The sampe was then croshed to a gravel size in the jaw crusher.

c) The crushed sample was then milled in a tungsten-carbide milling vessel, for one and a half to two minutes

d) Approximately 3-4 gms of the milled sample was heated for 3-4 hours at 110° C, to remove any moisture from the rock.

e) The sample was then ignited to a temperature of 960°C in the Neytech furnace for 12 to establish loss of volatile material.

f) 1 -1.10 gms of the ignited sample was added to 4- 4.10 gms of flux (Lithium Metaborate). The powder and flux was then fused into discs in a platinum-gold crucible at 1100°C. Ammonium iodide was used as the wetting agent. These discs were analysed by XRF to determine the major element composition of the samples.

g) Approximately 5 grams of unignited rock powder was mixed with up to 1ml of PVA solution, and using boric acid as a support medium pressed pellets were produced. These pressed pellets are analysed by XRF to determine the trace element composition of the samples

2. Analytical Method:

All whole rock analysis was carried out by the x-ray fluorescence technique.

2.1. Major Elements: The following major elements were analysed for: SiO_2, Al_2O_3, Fe_2O_3, MnO, MgO, CaO, Na_2O, K_2O, TiO_2, P_2O_5 and SO_3.

2.2. Trace Elements: The following trace elements were analysed for: Y, Sr, Rb, Nb, Zr, Th Pb, U, Ga Cu, Zn, Ba, Sc, V, Cr, Ni, Ce, Nd and La.

3. Mineral Separation:

Mineral separation for both micas, biotite and muscovite were carried out to determine Rb/Sr compositions for determination of the closure temperature and development of an age relationship in this rock type.

The procedure used was as follows:

a) The gravel sized jaw crushed sample was further crushed in the disc mill and sieved through a 500μ mesh. The less than 500μ portion was collected for the mineral separation by froth flotation.

3.1. Flotation

a) The sample was washed several times with tap water to remove any fines.

b) The Denver container was then refilled to just below its lip with water and up to 40 mls. of Armac T solution is added. The Armac T provides the bubbles which the mica flakes adhere to.

c) Once the Armac T has been added the pH of the solution needs to be lowered to 3 so that quartz will not float off as well.

d) The agitator is lowered into the solution and run vigorously for 10 minutes, this is done so all particles are coated with the Armac T.

e) After 10 minutes air is introduced via the air valve to facilitate bubbling, and the flotation process.

f) The "mica froth" was removed from the top of the flotation vessel into a fine nylon sieve. The Armac T and micas are separated by washing with detergent and water. The mica fraction containing both muscovite and biotite once retrieved was dried on a hotplate.

3.2 Magnetic Separation:

Having obtained the mica fraction it is possible to separate them on a Frantz magnetic by way of differences in their magnetic suceptabilities.

a) Non-magnetics such as quartz and feldspar are picked up and need to be removed. This is done by setting the magnetic field at 1.5 A with a 20° side angle and a 25° forward angle

b) This provides a sample consisting of a dominant mica fraction. The two micas are separated on a setting of 1.2 A, a side and forward angle of 25°, and feed speed of 8.

c) These samples were then selectively handpicked to remove any composite grains and improve sample quality.

4. Whole Rock and Mineral Separates Sr, Nd and Sm Preparation.

4.1 Weighing: 100 mg of sample is required for each, isotopic composition and isotopic dilution for whole rock analysis. As a result of this 200 mg of sample powder was weighed into a teflon beaker on the Sartorious 5 decimal place balance. A drop of 6N HNO_3 was also added to the beaker, which was then deionised using a Zerostat gun to remove any static charge present.

Mineral separates were treatedthe same way but more sample was weighed out, ~200 mg of the Biotite and ~300 mg of Muscovite.

4.2 Dissolution: a) 1 ml of 6N HNO_3 and 4ml of HF were added to the whole rock and left overnight at 180° C, and evaporated to dryness at this temperature the next morning.

b) Once evaporated another 1ml of 6N HNO_3 and 4mls of HF were added to the whole rock samples and left on the hotplate at 150° C for 5 days to allow complete dissolution of the sample. For the the mineral separates the process is the same except 5 drops of perchloric acid were added in addition to the HNO_3 and HF.

c) Following the 5 day period the sample was evaporated to dryness and 6mls of 6N HCl were added and kept at approximately 120° C and left to dissolve overnight.

4.3 Splitting and Spiking: The samples need to be split, so one fraction can be spiked for isotope dilution and the remaining pure fraction is kept for isotope composition.

a) A clean beaker is tared and labelled ID for isotope dilution.

b) The sample is poured into this and weighed, and the weight is recorded.

c) 3/4 of the solution is poured back into the original beaker, capped and labelled as IC.

d) The remaining solution is weighed again and recorded as the spiked solution weight.

e) The balance is tared and then spike is added and the weight recorded.

f) Samples are the evaporated to dryness and have 1.5mls of 3N HCl added to totally dissolve the sample.

g) The solution is then added to a centrifuge tube and centrifuged at 3000 rpm for 5 minutes. Theresultant supernatant solution is ready for addition to the ion exchange columns for the removal of Sr, Nd and Sm.

Appendix 4. Isotopic Parameters and Equations

The following section covers the constants, decay rates and equations used in Chapter 7, (from Schaefer, 1993).

	Rb-Sr	Sm-Nd
Decay Constant λ:	$1.42\pm0.01 \times 10^{-11}$	$6.54\pm0.05 \times 10^{-12}$
CHUR:	$^{87}Rb/^{86}Sr = 0.0827$	$^{147}Sm/^{144}Nd = 0.1966$
	$^{87}Sr/^{86}Sr = 0.70450$	$^{143}Nd/^{144}Nd = 0.512638$
Depleted Mantle:	$^{87}Sr/^{86}Sr = .7027\pm5$	$^{143}Nd/^{144}Nd = 0.5132\pm1$

Epsilon Nd: $\varepsilon^{t}_{Nd} = ((({}^{143}Nd/^{144}Nd)^{t}_{sample} / (^{143}Nd/^{144}Nd)^{t}_{CHUR}) -1) \times 10000$

Model Age: $T_{mod}^{CHUR} = 1/\lambda\ (m/((N/S) - (N/S)_{CHUR}) +1)$

N= number of atoms in the radiogenic isotope (^{87}Rb and ^{147}Sm)

S= number of atoms in the stable isotope (^{86}Sr and ^{144}Nd)

Appendix 5 :Trace Element Modelling of AFC Processes

Modelling of the AFC process was carried out using trace elements with a modified version of the original equation developed by Depaolo, 1981 from Wilson 1987. The equation used was:

$$C_L = C_L^o f + \frac{r}{r-1+D}.C*(1-f)$$

Where: C_L^o= the concentration of an element in the original magma

C_L = the concentration of the element in the contaminated magma

C*= the concentration of the element in the contaminant

r= the ratio of the rate of assimilation to the rate of fractional crystallisation

D= the bulk distribution coefficient for the fractionating assemblage

F= the fraction of the magma remaining

$f = F^{-(r-1+D)/(r-1)}$

The D values used came from various authors and were as follows:

D_{Zr} = .1995 (1)

D_{Nb}= .055 (2)

D_Y = .155 (2)

D_{Ce}= .1 (3)

The other parameters which were involved are:

	Clo (ppm)	C* (ppm)	Actual C_L (Rhyodacite ppm)
Zr	113	218	556
Nb	7.725	71.7	38.29
Y	29.625	28.2	75.56
Ce	33	68.8	117.6

(1) Wilson, 1987.

(2) Pearce and Norry, 1979.

(3) Cox et al., 1979.

Appendix 6

Sample Localities Maps

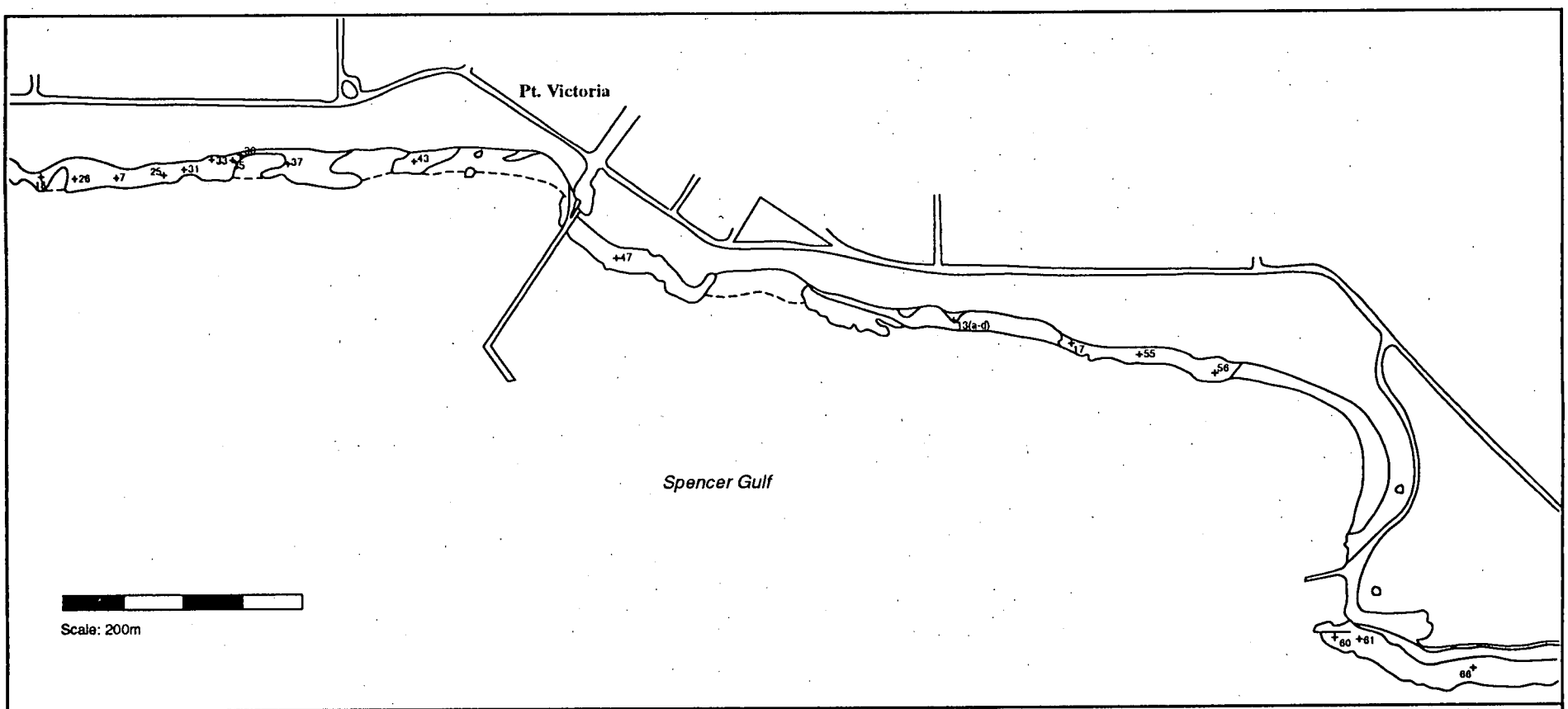

Locality Map showing the sites where analysed samples were taken from.

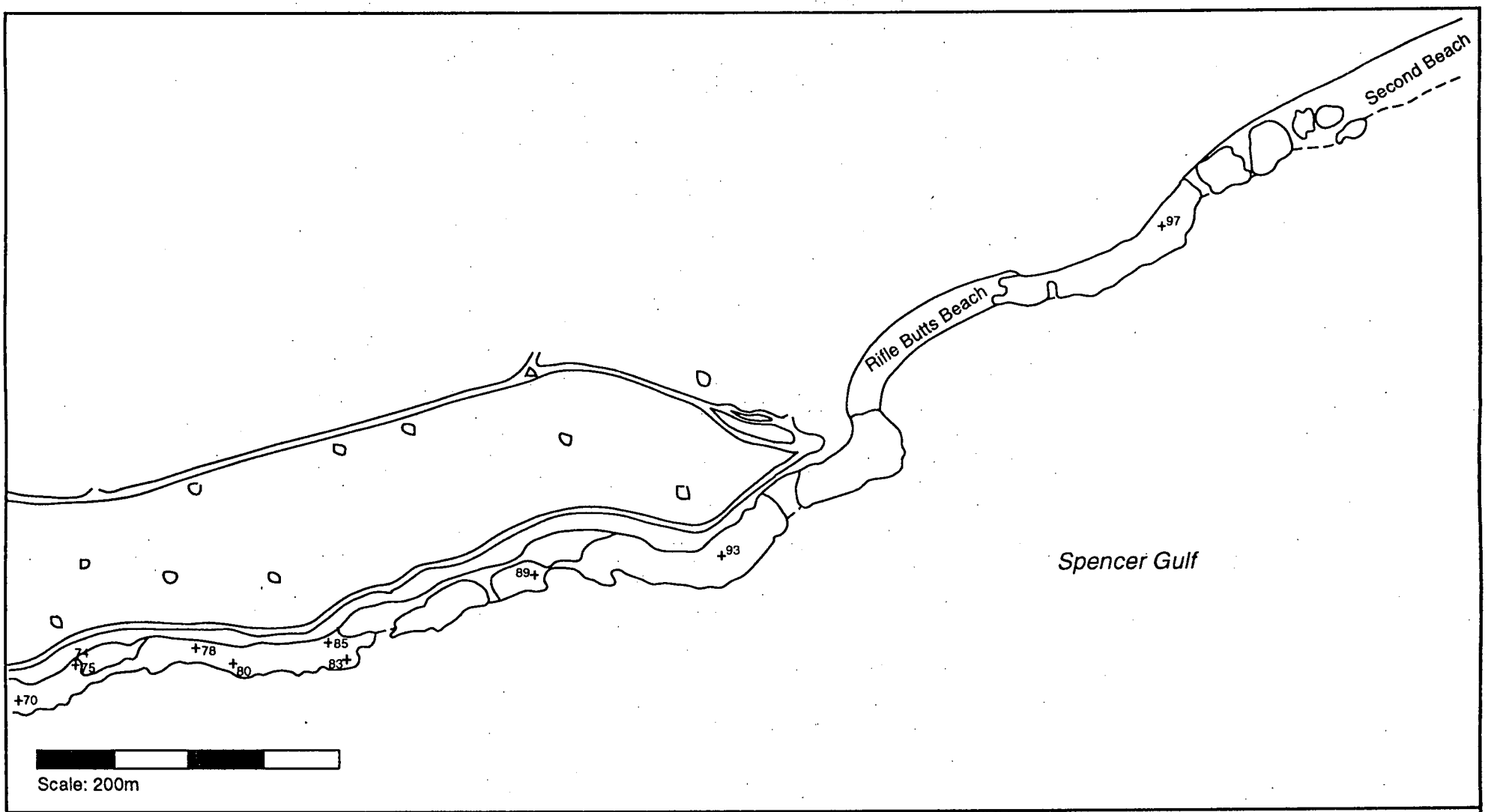

Locality Map showing the sites where analysed samples were taken

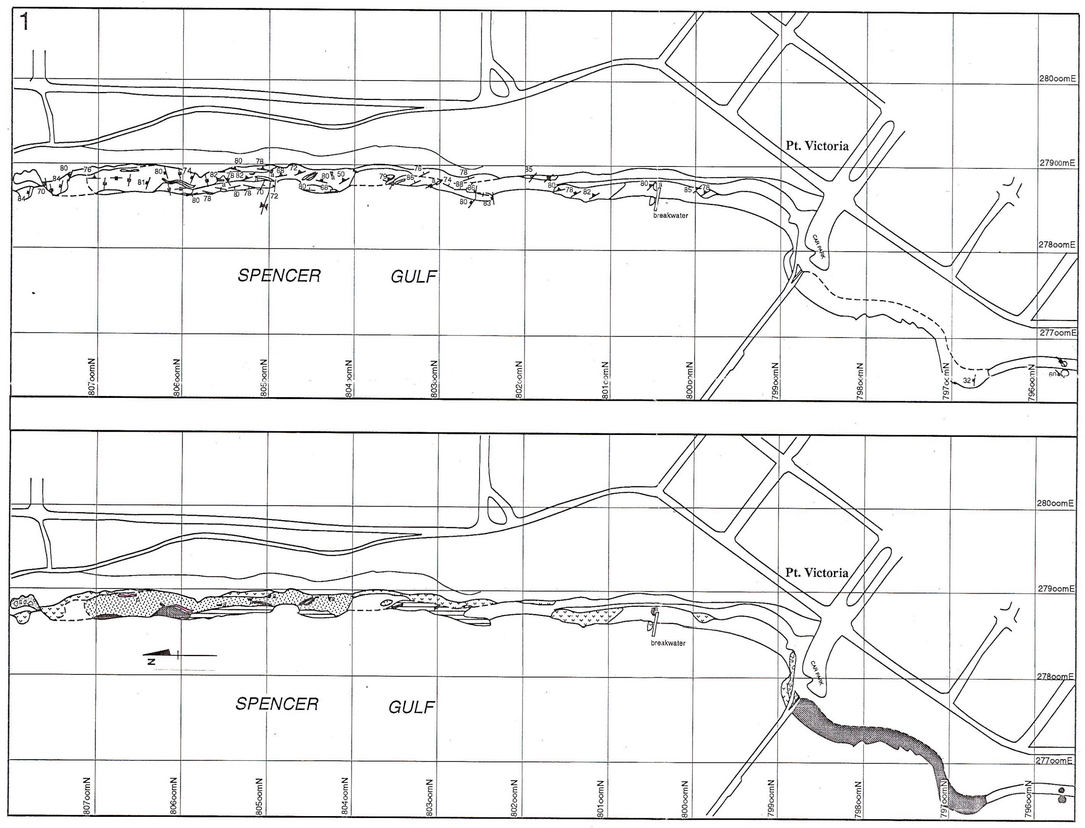

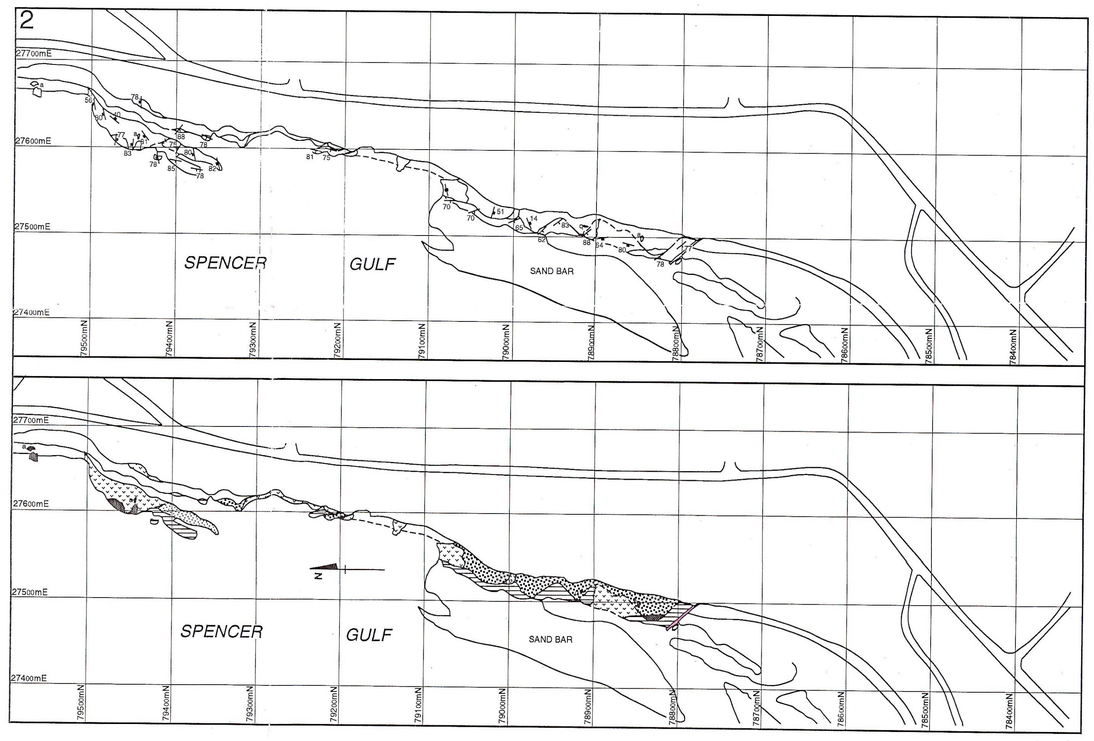

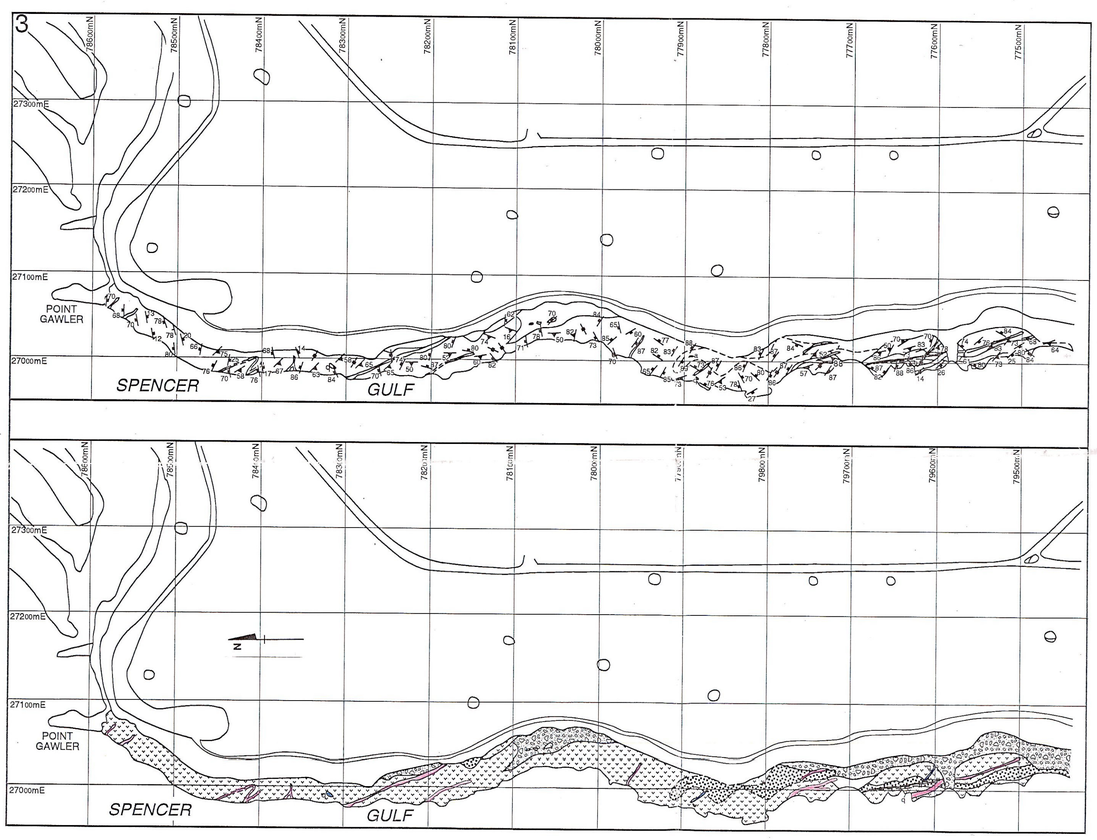

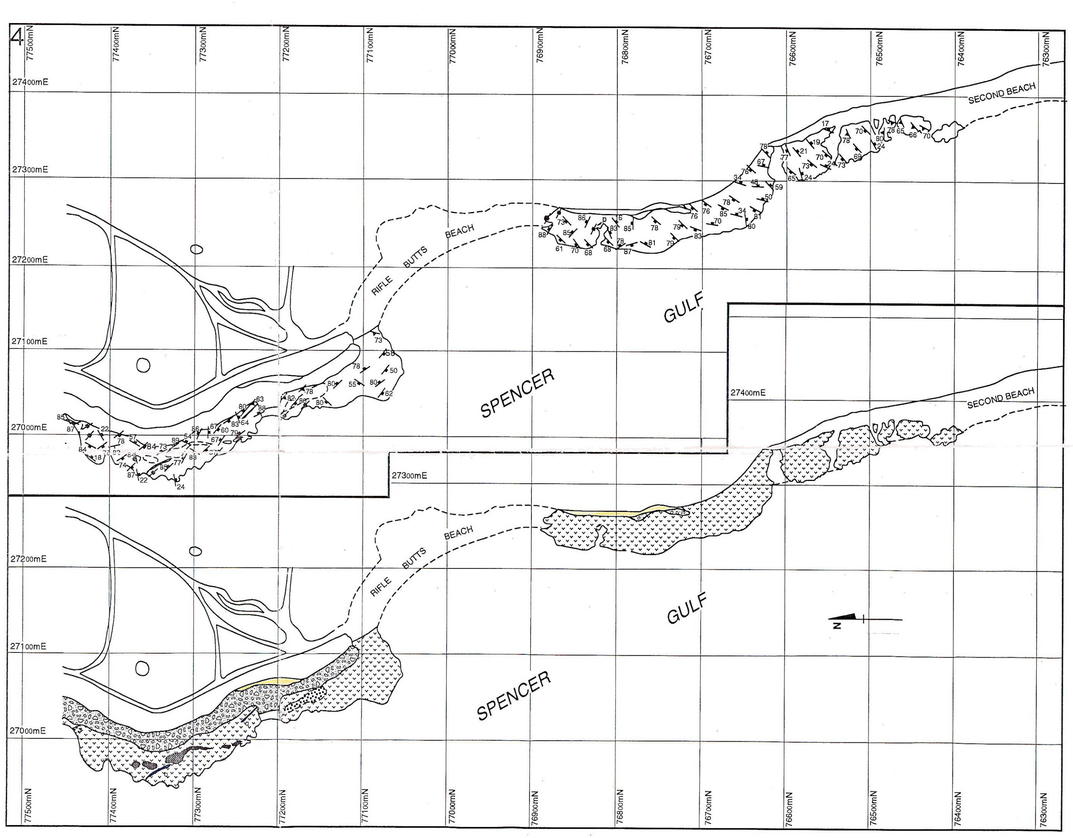

THE GEOLOGY OF THE PORT VICTORIA AREA

SOUTH AUSTRALIA

SCOTT HUFFADINE 1993

0 100 metres

LEGEND

Lithologies

- Calcrete
- Rhyodacite Scree
- Amphibolite intrusives
- Porphryitic Rhyodacite
- Hyaloclastite Breccia
- Metasediment - Massive unit
- Metasediment -Layered unit

Symbols

Foliation
- Inclined
- Vertical

Layering
- Inclined
- Vertical

Joints
- Inclined
- Vertical

- Fold axis (Syncline)

Lithological Boundaries
- Established
- Inferred

Miscellaneous
- Vein
- p-pegmatite
- q-quartz